NORTH-WEST UNIVERSITY
YUNIBESITI YA BOKONE-BOPHIRIMA
NOORDWES-UNIVERSITEIT

Synthesis and Characterisation of Ag / TiO_2 and Ag / TNT nanocomposites

By

Lesego Fortunate Metswamere (16876849)

B.Sc. Honours Chemistry (North-West University, South Africa)

A thesis submitted in fulfilment of the requirements for the Master's degree in

Chemistry

In the Faculty of Agriculture, Science and Technology

(Department of Chemistry)

North-West University : Mafikeng Campus

Supervisor: Dr Mbhuti Hlophe

Co-supervisor: Dr Lucky Sikhwivhilu

2012

DECLARATION

I_____ declare that this project which is submitted in fulfillment of the requirements for the degree of Master of Science in Chemistry (M.Sc.) at North West University, Mafikeng Campus has not been previously submitted for a degree at this university or any other university. The following research was compiled, collated and written by me. All the quotations are indicated by appropriate punctuation marks. Sources of my information are acknowledged in the reference pages.

..... ----------

Lesego Fortunate Metswamere Date

ACKNOWLEDGEMENTS

I would like to express my sincere appreciation to the following;

- God almighty for giving me strength and patience.
- My supervisor Dr M. Hlophe and co-supervisor Dr. Sikwhwivhilu for invaluable support, patience, guidance and inputs through-out the study.
- CSIR for letting me use their techniques and the staff for technical assistance.
- North-West University Chemistry laboratory technicians especially Mr. Mahlangu for their technical support.
- North-West University and department of chemistry for financing my trips to CSIR (pretoria).
- NRF scarce skills for financial support.
- My family; mom grandmother, aunt, uncles and my brother. For their love, support and encouragement.
- Professor Selvaratnam for contributions and encouragement.
- My friend and colleague Miss Seoposengwe for all the help and encouragement offered when was needed.
- Not forgetting the science centre team (Miss Molebatsi, Thato Majele and Miss Masenya) for their support and encouragement.
- Lastly I would like to thank myself for all the hard work.

ABSTRACT

Titanium dioxide (TiO_2) was prepared by wet chemical process (sol-gel) using titanium tetraisopropoxide (TTP) as the precursor and either a bioalcohol (methanol, ethanol or 1-butanol) or an inorganic base (ammonium hydroxide) as a solvent. The final products were then characterized using scanning electron microscopy (SEM), transmission electron microscopy (TEM), X-ray diffraction method (XRD), fourier transform infrared spectroscopy (FT-IR), and the Brunauer-Emmert-Teller method (BET). The surface areas of bioalcohols were found to be larger than that of ammonium hydroxide a weak inorganic base. This suggests that bioalcohols are more reactive than NH_4OH. The SEM data shows that increasing chain length of bio-alcohols leads to a formation of bigger particles with regular oval shape. The difference here is ascribed to alcohol solubility in water. Interestingly, the use of NH_4OH as a solvent in the sol-gel process led to the formation of relatively smaller particles than that obtained in the presence of bio-alcohols and these small particles formed a porous structure. This is attributed to the difference in pH. Since bioalcohols have larger surface areas and are therefore more reactive than ammonium hydroxide, then given the same time for reactions, bioalcohols mediated reactions should be faster and produce larger particles than is the case for ammonium mediated reactions. As was expected the formed xerogels were amorphous.

The powder samples obtained from the sol-gel process were then treated further by microwave heating to obtain different morphology like nanotubes. A very concentrated solution of Potassium hydroxide (KOH) solution was used to transform the morphology of the prepared samples. The final products were then characterized using techniques outlined above. The SEM results revealed that treatment of samples by KOH under microwave heating transformed the prepared TiO_2 materials into nanotubes. The XRD peaks of the microwave treated materials were sharper than those of the xerogels indicating that the tubular materials were more crystalline than the gels. Additionally, surface areas of the tubes obtained from BET were decreased and this was attributed to material transformation from xerogel to crystalline forms of TiO_2.

Two of the samples prepared by sol-gel method (SCM 1 and SCM 2) were calcined at 400 °C for 3 hours and then characterised before they were treated hydrothermally in a microwave. In order to control the phase composition of the materials four samples were calcined after microwave treatment. Obtained products were characterized using the instruments outlined

above. The XRD patterns for materials that were calcined at 400 °C after microwave treatment were similar to those obtained from microwave treatment suggesting that there is no structural change. This means that the tubes are thermally stable upto 400 ℃. samples that were calcined at 400 °C prior to microwave assisted hydrothermal processing, formed anatase TiO_2 with a high degree of crystallinity. The formation of anatase TiO_2 clearly shows that depending on the starting materials phase pure materials could be achieved. However, exposure to high temperatures led to particle growth by Ostwald ripening. The particle sizes showed a slight increase of about 16-24 nm as a result of crystal growth induced by thermal treatment.

It was found that silver supported on nanotubular titanate materials was well dispersed and had a larger particle size of about10 nm compared to TiO_2 materials obtained from the sol-gel process. This suggests that the tubular morphology facilitates the formation of silver and offers better interaction between nanotubes and silver nanoparticles. This may be due to the large surface areas of nanotubular materials.

TABLE OF CONTENTS

LIST OF ABBREVIATIONS

SEM- Scanning electron microscopy

TEM- Transmission electron microscopy

XRD- X-ray diffraction

FTIR – Fourier transform infrared spectroscopy

UV – VIS- ultra violet visible spectroscopy

KOH – Potassium hydroxide

NaOH – Sodium hydroxide

NH_4OH – Ammonium hydroxide

TiO_2 – Titanium dioxide or titania

TTP – Titanium tetraisopropoxide

Ag – Silver

Ag / TiO_2 – silver titanium dioxide

BET – Brunauer – Emmett – Teller method

EDX- Energy dispersive x- ray spectroscopy

RT- Room temperature

MW- Microwave prepared material

CMW- Materials sintered after microwave treatment

SCM- Materials calcined prior to microwave treatment

AGL Materials loaded with silver

LIST OF FIGURES

LIST OF TABLES

DEFINITION OF CONCEPTS

Nanotechnology- It is the understanding and control of matter at dimensions of 1-100nm where unique phenomena allow new applications.

Apatite- It is a group of phosphate minerals, usually referring to hydroxyapatite, chlorapatite, fulorapitite and bromapatite named for high concentration of OH^-,F^-,Cl^- or Br^- respectively in the crystal.

Band-gap- Is an energy range in a solid where no electron states exist.

Electron-hole pair- Is the fundamental unit of generation and recombination, corresponding to an electron transitioning between the valence band and the conduction band.

X-ray photoelectron spectroscopy- Is a quantitative spectroscopic technique that measures the elemental composition, empirical formula, chemical state and electronic state of the elements that exist within the material.

X-ray diffraction- Is a versatile, non-destructive technique that reveals detailed information about the chemical composition and crystallographic structure of natural and manufactured materials.

Doping- It is the process of introducing impurities into an extremely pure semiconductor to chang its electrical properties.

Nanocomposite- Is a multiphase solid material where one of the phases has one, two or three dimensions of less than 100 nanometers.

Calcination -Is a thermal treatment process applied to ores and other solid materials in order to bring about athermal decomposition, phase transition, or removal of a volatile fraction.

Sintering - Is a method for making objects from powder, by heating the material in a sintering furnace below its melting point until its particles adhere to each other.

Annealing - Is a heat treatment wherein a material is altered causing changes in its properties such as strength and hardness.

Degradation -is the chemical breakdown of materials by a physiological environment.

In- situ – Is a latin phrase meaning 'in the place'.

CHAPTER 1

GENERAL INTRODUCTION

1.1 Background

Nanotechnology is the science and engineering involved in designing, synthesizing, characterizing and making technological use of materials that are at a nanoscale [1]. Nanotechnology is a multidisciplinary field and is capable of improving many sectors. It can be applied in various fields such as information technology, biotechnology, pharmaceutical, electronics, scientific tools and industrial manufacturing processes, transportation, water and environmental purification and medicine. The awareness of nanotechnology was first made by a physicist Richard Feynman in his talk, "There's plenty of room at the bottom". Feynman's lecture implied that the manipulation of materials at the scale of atoms and molecules was possible [1, 2].

Nanotechnology has the ability to work at a very small scale which ranges from 1 to 100 nm [3]. One nanometre is equivalent to one billionth of a metre, which is equivalent to the width of 6 carbon atoms or 10 H_2O molecules. The width of one human hair is about 80 000 nm and a red blood cell is about 7 000nm in width [1, 3]. Generally, there are two approaches to building up nanoscale structures and devices: top-down; bottom-up approaches. Top-down involves the break- down of materials into small structures. Bottom–up is whereby materials are directly built from atoms, molecules and other nano–objects. At the nanoscale the properties of the materials are more useful than their macroscopic form.

Size is a very important aspect in nanotechnology, and the smaller the materials the more suitable they are for different nanotech applications [2]. This is because materials at a nanoscale offer special properties that enable nanotechnology applications to improve many technology and industry sectors, thereby improving the standard of living. For example, it can offer communication and information technology applications that provide faster systems that can store large amounts of information. In medicine it offers enhanced biological diagnostics and early detection of diseases, whereas, the pharmaceutical industry is focussed on direct treatment of appropriate drugs to the damaged or cancer cells.

Nanomaterials are manufactured by ceramics, polymers, organic materials and their composites. Nanomaterials include nanoparticles, nanoclusters, nanofibres, nanowires, nanofilms, nanotubes and many others. Both the top-down and bottom-up technologies can be used to synthesize with ordered and random nanotopographies [4]. Their small size exhibits increased surface area and surface roughness. These improved properties lead to physicochemical properties such as electrical, optical, mechanical catalytic and magnetic properties. The smaller the size of nanomaterials the better improved the properties.

Semiconductor nanomaterials can be applied in areas such as energy conversion, sensing, electronics, photonics and biomedicine. Most applications require nanomaterials with greater flexibility. In order to achieve this, parameters such as size, shape and surface area should be varied to control their properties [5]. A unique way of obtaining nanomaterials with improved properties is to fabricate hybrid nanomaterials. This is because their properties are better improved than those of single component nanomaterials. Hybrid materials include doped and composite nanomaterials. Among the semiconductors, TiO_2 is the most attractive, especially in photocatalysis. This is because it is stable, cheap to produce and is capable of degrading many organic pollutants due to the positions of its valence and conduction bands [5].

1.2 Introduction

Special properties such as biological and chemical inertness, strong oxidizing power, non-toxicity and its resistance against photo and chemical corrosion make titania a preferred semiconductor photocatalyst [6]. As a result of these properties, titania finds application in various areas including gas sensing materials, electrochromic devices, photo-degradation of organic pollutants in water [7] and air and energy storage devices [8]. The surface properties of TiO_2 can be changed or modified by addition of metals such as silver thereby improving on the inherent properties of TiO_2 [9]. Nanometer-sized silver particles are known to exhibit strong antimicrobial and antibacterial properties [10]. Silver is a suitable and non-toxic element which improves the TiO_2 bioactivity because of its antibacterial activity.

TiO_2 is commercially available and can also be synthesized in the laboratory using various methods including the sol-gel method. This method is relatively simple, inexpensive and produces homogeneous products. In this method hydrolysable alkoxides are obtained through the chemical synthesis of oxides. Various types of alkoxides produced include aerogels, xerogels, sonogels, cryogels and vapogels [11]. Sol gel produced materials are amorphous and require higher temperatures to be crystallized [12]. Among the synthesis parameters in the structure of TiO_2 the type of solvent used is very important. Different types of solvents such as alcohols and bases have been used. The role of alcohols in the sol-gel method is to start the hydrolysis and condensation reactions. Researchers have used different alcohols in the preparation of TiO_2 to study the effect of these alcohols in the preparation of TiO_2. The sol-gel method has been successfully used to synthesize TiO_2 derived nanotubes in the presence of templates such as organogel [13]. However, the removal of a template is a challenge.

Hydrothermal treatment is an alternative method for fabricating titania derived nanotubes. This method is simpler, cheaper and less time consuming [14]. Microwave hydrothermal assisted method can offer materials with improved microstructure and better physical and mechanical properties. This is because it offers direct heating of materials and heat is generated throughout the entire volume of the material. This technique provides fast reactions at a short period of time leading to nanomaterials with improved crystallinity, large surface area, uniform particle sizes and unique morphologies. Among the various morphologies that can be produced, nanotubes are the most preferred because they possess large surface areas which offer more room for reactions.

In this thesis, properties of TiO_2 (morphology, surface area structure and composition) were controlled using different preparation methods; sol-gel and microwave assisted hydrothermal method and the prepared materials were then subjected to calcination.

1.3 Problem statement

Despite its great properties such as biological and chemical inertness, strong oxidizing power and non-toxicity, TiO_2 has low photocatalytic efficiency that limits its use in air purification and water disinfection. The photocatalytic inefficiency is usually caused by TiO_2 that is non-crystalline, has a large particle size and a low surface area. It is therefore important to develop TiO_2 with good surface properties. In order to achieve this, suitable methods for the production of titania with controlled size must be developed. Additionally, the structure of titania can also be improved by incorporation of metal ions.

1.4 Objectives of the study

In order to improve on the properties of TiO_2 the following were be attempted:

i. Synthesis of TiO_2 materials with a large surface area by a simple sol-gel method.
ii. Synthesis of TiO_2 derived nanotubes with large surface areas and uniform diameters
iii. Determination of thermal stability of TiO_2 based nanomaterials
iv. Preparation of Ag/TiO_2 composite materials
v. Characterization of TiO_2 based nanostructures and Ag/TiO_2 nanocomposites
vi. Determination of the sizes of nanostructures

1.5 References

1. Sahoo, S.K., Parveen, S., Panda, J.J., (2007). *Nanomedicine: Nanotechnology, Biology, and Medicine*: The present and future of nanotechnology in human health care 3, 20– 31
2. Miyazaki, K., and Islam, N., (2007). *Technovation* : Nanotechnology systems of innovation An analysis of industry and academia research activities 27, 661–675
3. Roco, M. C., (2003). *Current Opinion in Biotechnology* : Nanotechnology: convergence with modern biology and medicine 14, 337–346
4. Yan, G., Chen, J., Hua, Z., (2009) *Journal of Photochemistry and Photobiology A: Chemistry:* Roles of H_2O_2 and OH radical in bactericidal action of immobilized TiO_2 thin film reactor: An ESR study 207, 153-159
5. Tan, T. T. Y., Yip, C. K., Beydoun, D., Amal, R., (2003) *Chemical Engineering Journal*: Effects of nano-Ag particles loading on TiO_2 photocatalytic reduction of selenate ions 95, 179-186
6. Yu, J., Yu, H., Cheng, B., Trapalis, C., (2009) *Journal of Molecular Catalysis A: Chemical*: Effects of calcinations temperature on the microstructures and photocatalytic activity of titanate nanotubes 249, 135-142.
7. Behnajady, M. A., Eskandarloo, H., Modirshahla, N., Shokri, M., (2011). *Journal of Desalination* : Investigation of the effect of sol-gel synthesis variables on structural and photocatalytic properties of TiO_2 nanoparticles 278, (10 - 17)
8. Wang, D., Zhou, F., Liu, Y., Liu, W., (2008) Materials Letters : Synthesis and characterization of anatase TiO_2 nanotubes with uniform diameter from titanium powder 62, 1819 - 1822
9. Shahab, A. A., Mohammad, P., Azarmidokht, H., (2009) *Powder Technology* : Synthesis of TiO_2-Ag nanocomposite with sol-gel method and investigation of antibacterial activity against E.coli 196, 142-245
10. Zhang, J., Wang, Y., Yang, J., Chen, J., Zhang, Z., (2006) *Materials Letters* : Microwave- assited synthesis of potassium titanate nanowires 60, 3015-3017
11. Brinker, C. J., and Scherrer G. W., (1990) Sol-gel science : The physics and chemistry of sol-gel processing,
12. Wang C. C., and Ying, J. Y., (1999) *Chem. Mater* : Sol-gel synthesis and hydrothermal processing of anatase and rutile titania nanocrystals, 11, 3113-3120

13. Yu, J., and Yu, H., (2006) *Materials Chemistry and Physics* : Facile synthesis and characterization of novel nanocomposites of titanate nanotubes and rutile nanocrystals 100, 507 -512
14. Qamar, M., Yoon, C. R., Oh, H. J., Lee, N. H., Park, K., Kim, D. H., Lee, K. S., Lee, W. J., Kim, S. J., (2008) *Catalysis Today* : Preparation and photocatalytic activity of nanotubes obtained from titanium dioxide 131, 3 -14

1.6 Dissertation outline

Chapter 2 (Literature review)

In this chapter, titania and titania derived nanomaterials are discussed, i.e. definition, types and applications are given. This chapter discusses the advantages and limitations of titania nanomaterials. Silver nanoparticles which can solve the problems associated with the applications of titania nanomaterials are included. Methods that can improve the properties of titania nanomaterials are also included.

Chapter 3 (Experimental procedures)

This chapter outlines the experimental procedures that were employed to achieve the objectives of the study.

Chapter 4, 5, 6 and 7 (Results and discussion)

These chapters tackle the results, discussions and conclusions of the study. Synthesis and characterization of titania nanomaterials are given in detail.

Chapter 8 (General conclusions and recommendations)

Conclusions based on the interpretation of results from chapters 4, 5, 6 and 7 are drawn. Recommendations for future work are brought forward.

CHAPTER 2

Literature Review

2.1 Introduction

Titanium dioxide (TiO_2) is the most used single crystalline material in surface science and the most widely used semiconductor in photocatalysis [1, 2]. This is because of its unique properties such as chemical and thermal stability, strong oxidizing power, non-toxicity, unique electronic properties and its resistance to chemical breakdown [1,3]. Its chemical and physical properties highly depend on the morphology, particle size and crystal structure. TiO_2 is the most active photo catalyst under the photon energy $300nm < \lambda < 390nm$ and remains stable after repeated cycles of catalysis [4]. It has the following important features for heterogeneous photo catalysis, (1) ambient temperature and pressure; (2) the ability to mineralize parents and their intermediate compounds without secondary pollution and (3) low cost.

Titanium dioxide occurs in three major crystalline structures; anatase (tetragonal) rutile (tetragonal) and brookite (orthorhombic).[5,6,7] These crystalline structures differ in their refractive index, dielectric constant and chemical and photo chemical reactivity. Nevertheless, only anatase and rutile are involved in the applications of TiO_2. The crystalline structure of TiO_2 is related to its photocatalytic activity. [8] Anatase has a high photocatalytic activity because it has higher electron mobility, lower fixed dielectric properties and a lower density than other crystalline structures. Rutile is the thermodynamically most stable. Other structures, such as the orthorhombic α-PbO2-type phase and the monoclinic baddeleyite phase exist [9]. These structures may be stabilized only under high pressure from a starting material of either anatase or rutile. A single crystal of anatase, for example, undergoes the following sequence of structural transitions under high pressure:

anatase ($I4_1/amd$) ⟶ α-PbO_2-type phases ($Pbcn$)

⟶ baddeleyite ($P2_1/c$)

The particle properties of TiO_2 such as particle size, crystallinity and phase purity depend on the method of synthesis, synthesis conditions and precursors. For this reason, it is difficult to control the particle properties of TiO_2. The performance of TiO_2 depends on the surface area to volume ratio because in most cases, the interaction between TiO_2 and the interacting media

takes place on the surface of these materials. The photocatalytic properties of TiO_2 also depend on its crystalline structure, morphology and crystallinity [10].

In order to synthesize TiO_2 materials with the above mentioned properties, a simple method for the synthesis of nanosized TiO_2 must be developed. The sol- gel method is widely used because it is versatile, easy to use and produces homogeneous and high purity materials [11, 12]. Optimal synthesis conditions of the sol-gel method for the preparation of TiO_2 have been reported. Wang and co-workers used the sol-gel method to examine the processing parameters in wet-chemical method that controls the crystallite size and phase of the nano – TiO_2 materials [13]. Qiu and co-workers developed an easily controlled sol-gel process to synthesize nano-sized TiO_2 by hydrolyzing TTP in the mixture of isopropanol and de-ionized water [11]. Behnajady and co-workers investigated the effect of calcinations temperature, solvent type and precursor on the crystallinity, particle size and photocatalytic activity of TiO_2 nanomaterials by the sol-gel method [14].

Due to its wide band gap, TiO_2 can only be activated by near-UV radiation which constitutes a very low percentage of the natural sunlight [15]. Additionally, the recombination of electron hole pairs is a problem because it constitutes low quantum yields. For better photocatalytic efficiency, TiO_2 photoresponse can be increased by shifting its adsorption to the visible light region and the recombination of electron and holes should be prevented. These can be achieved by incorporating metals onto TiO_2. To narrow the bandgap, ions have been doped into the crystal lattice of TiO_2 and the doped TiO_2 is more sensitive to visible light [15]. The recombination of electron and holes has been tackled by depositing metals such as Pt, Ag and Au on the surface of TiO_2. This prevents the electrons from recombining with the holes by mediating the electrons away from the surface of TiO_2.

2.1.1 Applications of TiO_2

Titanium dioxide finds many applications such as waste water treatment, air purification and medical treatment [16]. Various studies have demonstrated that TiO_2 achieves these treatments through the deactivation of bioparticulates. Bioparticulate is the term that describes bacteria, viruses, prions and cancer cells. The antibacterial activity of TiO_2 based photocatalysis depends on factors such as bacterial strains, light source, irradiation time, photocatalysts type, concentration of contaminants and others [17]. It has been found that nano-sized TiO_2 particles

have better photocatalytic activity than its bulk material. Among the three known forms of TiO_2, anatase and rutile are the most commonly used in photocatalysis. However, anatase is known to have a greater photocatalytic activity than rutile. Additionally, earlier reports have demonstrated that a mixture of both phases consisting of 70 - 75 % anatase and 25 – 30 % rutile is better than a single phase [17]. Titanium dioxide photocatalysis is limited to environments with sufficient UV light and this affects its photocatalytic activity. Parameters such as phase composition and addition of dopants can be used to improve the photocatalytic activity of TiO_2 [18]

2.1.2 The synthesis methods of titanium dioxide nanomaterials

The physical and chemical properties of TiO_2 are largely influenced by their particles size, morphology and crystallinity [19]. The sol-gel method allows for compositional and microstructural tailoring of TiO_2 by controlling the starting conditions. Factors affecting the sol-gel process include the reactivity of alkoxides, pH of the reaction medium, H_2O: alkoxide ratio, reaction temperature and nature of solvent used. Variation of these parameters results in materials with different microstructure and surface chemistry [19]. However, the sol-gel processed materials are typically non-crystalline and often require post thermal treatment to achieve the required crystallinity levels, but this leads to a significant compromise in the surface area.

Behnajady and co-workers synthesized titanium dioxide nanoparticles by the sol-gel method. The synthesis was done using different precursors (i.e. titanium n-butoxide and titanium tetraisopropoxide) and solvents (methanol, ethanol and isopropanol) under different conditions such as solvent quantity, reflux temperature, reflux time, sol drying method and calcination temperature. The results revealed that crystallinity of nanoparticles depends on the synthesis conditions [14]. When the solvent with a higher polarity such as methanol is used as a reaction media, the rutile phase content and the crystallite size increase. This implies that a solvent with a higher polarity accelerates condensation and hydrolysis reactions [14]. Increase in reflux temperature results in reduction of rutile phase content and increase in anatase phase content. Also the crystallite size of anatase and rutile decreases with increasing the reflux temperature. These results show that the reflux temperature is effective in the crystallite size and amount of each phase of TiO_2 nanoparticles. Increasing the calcinations

temperature resulted in the increase in crystal size of both phases and increase in rutile phase content.

C. Su and co-workers investigated microstructural and chemical properties of TiO_2 prepared by the sol-gel method. A portion of the as-synthesized samples was calcined at a temperature range of 400° C to 700° C. From the XRD results, at 400° C only the anatase phase was observed and at 700° C the rutile phase became dominant. The XRD also showed that the crystal size increased with an increase in temperature due to crystal growth [19]. In contrast, according to the BET the surface area decreased as the temperature was increased due to increase in crystal size [19]. The photocatalytic activity of TiO_2 was studied through the photodecomposition of salicylic acid. After the analysis it was found that the anatase phase products showed a high photocatalytic activity. It was also found that the calcination temperatures used after the sol-gel preparation of TiO_2 samples greatly affects the photocatalysis efficiency of samples in the photodecomposition of salicylic acid [19,20]

In most cases, rutile phase of TiO_2 is obtained by sintering of the material [21]. However, a different approach was carried out by Wang and co-workers whereby the anatase and rutile phases were successfully synthesized in mixed organic media with the variation of alcohols under mild conditions. It was found that the phase, partial morphology and size of TiO_2 particles are influenced by the type of alcohol used and temperature. For example, synthesis with ethanol (liquid phase 1) at 100° C resulted in rutile phase with the crystal size of 6 nm, whereas synthesis with ethylene glycol (liquid phase 2) at 100° C resulted in the formation of anatase phase with the crystal size of 4.5 nm and when the temperature for both materials was increased to 150° C, crystal sizes were increased to 10 and 5.2 nm respectively. Additionally, when glycerol (liquid phase 3) at 100℃ was used, amorphous materials were obtained but when the temperature was increased to 150℃, materials crystallized into rutile phase with crystal size of 6.5 nm. The epitaxial growth which was indicated by thin line width could be observed on the diffraction planes of pure rutile TiO_2 produced in liquid phase 1. These results show that ethanol is more reactive than the other two used alcohols. The formation of titania in these systems is based mainly on the hydrolytic process initiated by the water generated as a result of esterification reaction between the alcohols and acetic acid [21].

The synthesis of ultrafine TiO_2 nanoparticles with tailored, crystal phase and size and thermal stability was carried out [22]. To achieve a very narrow particle size distribution in the desired range, Wang and co-workers examined the water: alkoxide ratio as a synthesis parameter to control the rates of nucleation and growth of clusters. High water: alkoxide ratios were found to favour the formation of ultrafine titania particles. Materials were first prepared by sol-gel method followed by hydrothermal treatment or calcination. Nanocrystalline anatase TiO_2 particles with grain size in the range of 5 to 100 nm were obtained via sol-gel and further treated under hydrothermal conditions followed by calcination. The resultant nanoparticles exhibited small particle sizes, few agglomerates and excellent thermal stability [22]. High water content ensured proper hydrothermal treatment of amorphous gel to promote nucleation of nanocrystals. These conditions allowed an ultrafine crystallite size to be obtained, especially at low hydrothermal temperature where particle growth was minimal [22].

Treatment of amorphous titania can result in the production of anatase. The anatase phase has a large surface area than the rutile phase which is a very important property. It is therefore important to stabilize the anatase phase without affecting its properties. Control over the hydrothermal conditions as well as over the contaminant ions present after the amorphous titania production are important to control the crystallization properties of the anatase powder [22]

An amorphous titania was treated hydrothermally in order to crystallize it into a stable anatase phase. To control the physical properties of the anatase powder, Ovenstone and co-workers varied hydrothermal treatment conditions such as temperature, pH and time. Samples produced in the autoclave at higher temperatures for longer times and higher pH conditions resulted in a more stable anatase. Materials prepared at lower temperatures for shorter times under low to neutral pH resulted in the formation brookite. The presence of small quantity of brookite is reported to accelerate the phase transition from anatase to rutile [23]. Crystallite size also plays an important role in stabilizing the anatase phase. Thus, the larger the crystallite size the more stable the anatase phase is [23]. It is reported that the synthesis conditions such as temperature, time and pH play an important role in determining the final phase of the material.

Yanagiswa and co-workers [24] carried out a study to control the crystallization of anatase from amorphous titania using the hydrothermal technique. Different precursors ($TiCl_4$ and Ti

$(OC_2H_5)_4$) under different pH and temperature, were used. Materials prepared from TiCl4 containing the chloride ion showed a high intensity anatase peak, whereas materials prepared from the other precursor which lacked the chloride ion did not have this peak, implying that the chloride ion accelerates the crystallization of the anatase phase. The acidic conditions resulted in the formation of anatase, brookite and rutile, whereas the basic conditions accelerated the production of anatase phase. The materials treated at higher temperatures for longer times produced large crystal sizes.

2.2 Titania nanotubes

Different TiO_2 nanomaterials such as nanorods, nanowires, nanospheres, nanobelts and nanotubes are known to improve the performance of TiO_2 in photocatalyitc applications. This is because they have excellent catalytic, electronic, magnetic and mechanical properties [21]. Their different applications are related to their shape and size. In preparing these nanomaterials, it is important to understand their mechanism of formation. Titania nanotubes are the most applicable in photocatalysis because they have better physical and chemical properties. These properties include large surface area, high pore volume, high interfacial charge transfer rate and ion-changeable ability [16, 25, 26, 27]. "The transfer of charge carriers along the length of titania nanotubes can reduce the length of positive electron and hole pair" [25]. Titania has a semiconducting behaviour that produces very strong electronic interaction between titania nanotubes and their catalysts. As a result of this, catalytic activity increases hence the performance of TiO_2 nanotubes. The ability of nanotubes to withstand heat treatment makes their application in photocatalyisis very attractive.

2.2.1 The synthesis methods of titania nanotubes

TiO_2 nanostructures with either anatase or rutile structure can be synthesized hydrothermally using either commercially produced or laboratory synthesized TiO_2 nanopowders. When exposed to heat treatment, the product material can be transformed into a new crystalline phase [28].

Kasuga and co-workers hydrothermally [29] treated the sol-gel derived nanomaterials chemically using an aqueous solution of NaOH, followed by neutralization with HCl. The product was then washed with distilled water. The aim was to develop a new method for the synthesis of TiO_2 nanotubes with improved properties. From the BET results, the specific

surface area of the as-prepared materials was 150 m^2/g after hydrothermal treatment the surface area of the obtained tubes was greatly increased to 400 m^2/g. The needle-shaped nanotubes had a diameter of about 8 nm and a length of about 100 nm. These results prove that titania nanotubes with an increased surface area can be successfully synthesized by hydrothermal treatment.

P 25Degussa TiO_2 was treated with an aqueous solution of NaOH hydrothermally to produce titanate nanotubes. The formed titanate nanotubes were then treated with H_2SO_4 and then calcined at temperatures ranging from 400 to 700 °C. The nanotubes were well dispersed with a diameter of 6 – 12 nm. The XRD pattern revealed that at 400 °C materials were amorphous. At 500° C to 700° C peak intensities of the anatase phase increased, indicating an improvement in phase crystallization. Sulfate ions could stabilize the anatase phase at 700 °C. Surface area and pore volumes were found to be much larger than that of Degussa P25. At temperatures above 700 °C surface area and pore volume decreased and the sulfate ions were decomposed [30]

A new method for the synthesis of TiO_2 nanotubes was developed. Kasuga and co –workers treated either anatase or rutile phase TiO_2 with an aqueos solution of NaOH. Materials were then treated with an aqueous solution of HCl and washed with distilled water. The resultant TiO_2 nanotubular materials were needle-shaped with a diameter that was 8 nm and a length of 100 nm. The formation mechanism of the nanotubes was discussed. The crystalline raw material was first converted to an amorphous product through alkali treatment. Consequently titania nanotubes were formed after treatment with distilled water [31].A project on the synthesis of anatase TiO_2 nanotubes with a uniform diameter was carried out.

Liu and co-workers [32] prepared the nanotubes using hydrothermal treatment method followed by acid treatment and calcinations. The TEM results revealed that the nanotubes had an inner diameter of 3-4 nm with an outer diameter of 9-10 nm. Before and after post-treatment, the morphology of the tubes was the same but the compositions were proven to be different by the XRD. Before calcination the peaks of the nanotube were not very fine [32]. The as-prepared materials presented peaks which could be indexed to sodium titanium oxide, and the peaks after acid treatment were indexed to hydrogen titanium oxide. After calcination at 400 °C, the XRD patterns were highly crystalline and all the sharp peaks could be indexed

to the anatase phase. It was found that titanium dioxide nanotubes could be successfully synthesized by hydrothermal treatment without the use of a template. A mechanism for the formation of anatase TiO_2 nanotubes was also studied. Nanotubes are formed during the solvothermal process, and the compositions are changed by subsequent ionic exchange and dehydration under high temperature [32]. It was then concluded that the post acid and heat treatment alter the compositions of the nanotubes and do not remodel their framework.
A simple one-step hydrothermal reaction using alkaline solution has been developed to synthesize low-dimensional titanate nanostructures [33]. The processing parameters such as the structure of raw material, the nature and concentration of alkaline solution, reaction time and temperature control the morphologies of the resultant materials [33,34].

Sikhwivhilu and co-workers [35] reported on the influence of bases, base strength and effect of temperature on the preparation of TiO_2 derived nanostructures using hydrothermal synthesis method. This could yield materials with unique morphologies, small crystal sizes and large surface areas [35]. The effect of the nature of the base and the concentration of the base on the transformation of nanostructures were investigated using different techniques. Nanostructures were prepared using KOH, NaOH, LiOH and NH_4OH bases at different temperatures. The shape, nature and yield of formed nanostructures depended on the type and concentration of a base used as well as the temperature applied. Among the mentioned bases KOH was found to be more reactive because it produced nanostructured materials with different shapes. However, the shape and nature of the obtained nanostrutured products depended on the concentration of KOH whereas the yield of nanostructures depended on the temperature and concentration of KOH.

Yu and colleague [36] treated Degussa P25 TiO_2 with NaOH hydrothermally to obtain one dimensional titanate nanotubes and zero dimensional rutile nanocrystals. This was done by treating Degussa P25 TiO_2 with NaOH. The prepared samples were hydrothermally treated in an autoclave at 140 ℃ at different times. This resulted in the formation of tubes with a narrow size distribution and diameters around 8 – 10 nm. Small rutile nanocrystals were attached on the inner and on the outer surface of the titanate nanotubes. As the reaction time was increased, the surface areas and pore volume of the materials were increased. This was due to the fact that the rutile nanoparticles were steadily turned into tubular nanocomposites and finally completely formed titanate nanotubes [36].

Microwave–assisted hydrothermal synthesis serves as a preferred alternative in the production of titania nanotubes under controlled reaction parameters including temperature, pressure and time. Borkar and co-workers [37] studied the influence of microwave heating on the phase trans- formation of TiO_2 from anatase to rutile. The same samples were treated conventionally under identical conditions. The results indicated a complete transformation of rutile from anatase phase at 900 °C for 30 minutes in the microwave system. On the contrary, conventional treatment showed only a partial transformation to rutile at 1 000 ° C for 30 minutes. This proves that microwave accelerates phase transformation at lower temperatures, thereby saving energy. However, when the anatase samples that contain rutile were at 800 °C in both the microwave and conventional system the phase transformation was accelerated. This proves that the presence of rutile in the anatase accelerates complete rutile transformation.

Wu and co-workers [38] investigated a novel method for the synthesis of TiO_2 nanotubes by microwave irradiation. To obtain TiO_2 nanotubes, anatase or mixed phase titania was reacted with NaOH under a power of 195 W. The resultant tubular materials had the central hollow, open ended and multi-wall structure. The diameters of the nanotubes were about 8 to 12 nm with a length of 200 to 1000nm. These results showed that TiO_2 nanotubes could be obtained under certain microwave power at a short period of time under low temperatures. Based on the results it was then concluded that microwave irradiation has the advantage of uniform, rapid and volumetric heating.

2.2.2 The effect of calcination temperature on hydrothermally treated titania nanotubes

The calcination process affects the microstructures of titania nanotube products and also induces the phase transformation of titania nanotubes to the anatase phase [38]. Researchers have investigated the effect of calcination on the phase transformation, crystallinity, pore size and volume as well as the surface area of titania nanotubes. At 400 °C crystallinity advances and the anatase phase start to surface [39,40]. However, the anatase phase is thermally unstable and only persists up to a temperature of 600 ° C. The anatase phase of TiO_2 nanotubes prepared by hydrothermal treatment transforms into rutile at a temperature range of 600 – 800 ° C. Nevertheless, at this temperature range the morphology of the tubes gets transformed into nanorods. Above 800° C the length of the nanorods decreases as the width increases [38].

As the calcination temperature increases the crystal size and pore size also increase while the surface area and pore volume decrease. Based on the research findings, it is safe to conclude that calcination greatly affects the crystallinity, morphology, pore structure and specific surface area and phase transition of titania nanotubes [38].

Yu and co-workers investigated the effect of calicination on the microstructures and morphology of titanate nanotubes. The nanotubes were prepared by hydrothermally treating P25 Degussa TiO_2 in the presence of NaOH followed by calcination of the resultant material at various temperatures. The XRD results revealed that materials calcined at 300 to 600° C crystallized into the anatase phase. At 700° C a mixture of both anatase and rutile was obtained and a complete phase transformation to rutile was observed at 800° C. As the calcinations temperature was increased from 400 to 900° C, the surface areas were decreased significantly. This was attributed to be due to complete transformation into the rutile phase and growth of TiO_2 crystallites [39]. The SEM results revealed that as the calcination temperature was increased the particles became more agglomerated resulting in a wider diameter of particles. It was then concluded that the calcinations temperature affects the crystallinity, morphology and surface area of TiO_2 nanotubes [39].

A study on the effect of calcination on the crystallinity of TiO_2 nanopowders was carried out. Chen and co- workers prepared the nanopowders prepared using titanium tetraisopropoxide (TTP) as a precursor in varied pH aqueous solution containing surfactants. The samples were calcined at the temperature range of 250 to 900° C. From the XRD results it could be seen that all samples were crystalline with anatase at a temperature range of 250 to 500° C. According to Chen and co-workers, this is lower than the results obtained from literature. This might be due to the preparation conditions [40].The rutile phase started to emerge at 600 and at 900° C a complete rutile transformation was observed. Based on the results it was then concluded that nanocrstalline TiO_2 can be successfully synthesized by hydrolysis of TTP in the presence of surfactants.

2.2.3 Formation of titania nanotubes

Methods such as the assisted-template method and hydrothermal treatment are presently used for the production of titanium dioxide nanotubes [22]. The hydrothermal treatment is one of the most applied methods that can yield low dimensional [43] well separated and crystallized

nanotubes that are suitable for large scale production [40]. This method has advantages such as high reactivity, simple control of the aqueous solution and usage of minimal energy. In hydrothermal synthesis, titania nanotubes are produced by reacting titania nanopowders with an alkaline aqueous solution. Temperature also plays an important role on the formation of titania nanotubes. Titanate nanotubes are formed in the temperature ranging from 100 to 180° C [45]. Nanotube formation decreases when the synthesis temperature is outside the 100 and 180° C range [44]. At temperatures below 100° C there is no tube formation, also at temperatures above 180° C the formation of nanorods is favoured [40]. Studies have reported the best yield and high purity of titanate nanotubes between 130 and 150° C. For instance Sikhwivhilu et al. reported 100 % tube formation with a uniform diameter, large surface area and large pore volume at 150°C.

2.4 Silver

Pure silver is ideally ductile and malleable and has the highest electrical and thermal stability of any metal as well as the lowest contact resistance. It can act as an electron trap and promote the interfacial charge transfer processes in composite materials. Silver nanoparticles are prepared by biological or chemical reduction of silver salt [44,45]. Like titania nanoparticles, silver nanoparticles also have unique electrical, optical and biological properties. Hence, silver nanoparticles are applicable in catalysis, biosensing, imaging, drug delivery, chemical sensors, optical devices, nanodevice fabrication and medicine [42,21,43]. Metal nanoparticles including Cu and Zn have long been used as antibacterial agents, but among them silver has proven to be the most effective because it has good antimicrobial efficiency against bacteria, viruses and eukaryotic micro-organisms [41,46,47,48]. Ag nanoparticles deposited on inert, semiconducting materials appear to be good electrocatalysts for the oxidation of organic molecules. This is because at a nanometer scale these particles have a high surface area and interface-dominated properties [14]. Silver nanoparticles are prepared by biological or chemical reduction of silver salt [49,50]. Like titania nanoparticles, silver nanoparticles also have unique electrical, optical and biological properties. Hence, silver nanoparticles are applicable in catalysis, biosensing, imaging, drug delivery, nanodevice fabrication and medicine [47].

2.4.1 Mechanism of action of silver nanoparticles

The silver nanoparticles prepared from $AgNO_3$ show efficient antimicrobial property compared to nanoparticles prepared from other salts due to their large surface area, which provides better contact with microorganisms [51]. The nanoparticles get attached to the cell membrane and also penetrate inside the bacteria. The bacterial membrane contains sulphur containing proteins and the silver nanoparticles interact with these proteins in the cell as well as the phosphorus containing compounds like DNA [52]. When silver nanoparticles enter the bacterial cell it forms a low molecular weight region in the centre of the bacteria in which the bacteria co-glomerates thus, protecting the DNA from the silver ions. The nanoparticles preferably attack the respiratory chain, cell division finally leading to cell death. The nanoparticles release silver ions in the bacterial cells, which enhance their bactericidal activity [52].

2.4.2 Effect of size and shape on the antimicrobial activity of nanoparticles

The surface plasmon resonance plays an important role in determining the optical absorption spectra of metal nanoparticles, which shifts to a longer wavelength with the increase in particle size. The size of the nanoparticle implies that it has a large surface area to come in contact with the bacterial cells hence it will have a higher percentage of interaction than bigger particles [52,53]. The nanoparticles smaller than 10nm interact with bacteria and produce electronic effects, which enhance the reactivity of nanoparticles. Thus, it is corroborated that the bacterial effects of silver nanoparticles depend on size. The antimicrobial efficiency of the nanoparticle depend on the shapes of nanoparticles also, this can be confirmed by studying the inhibition of bacterial growth by differentially shaped nanoparticles. According to Pal et al. (2007), truncated triangular nanoparticles show bacterial inhibition with silver content of 1μg. While, in case of spherical nanoparticles total silver content of 12.5μg is needed. The rod shaped particles need a total of 50 to 100 μg of silver content. Thus, the silver nanoparticles with different shapes have different effects on bacterial cell.

2.5 Silver and Titanium dioxide

Silver is a suitable and nontoxic element which improves the TiO_2 bioactivity because of its inborn antibacterial activity against microorganisms. Bacterial growth inhibition in low concentration of silver and also good distribution of silver on titania makes titania an appropriate matrix for titania antibacterial agent. Production of silver in nanoranges results in

the generation of high surface area which is a significant property for bacterial inhibition. In addition, titania nanosize particles create more hydroxyl groups than micro-sized particles [48]. Silver can trap the excited electrons from TiO_2 and leave the holes for the degradation reaction of organic species. This also results in the extension of their wavelength response towards the visible region. Additionally, silver particles can facilitate the electron excitation by creating a local electric field and Plasmon resonance effect in metallic silver particles shows a reasonable enhancement in this electric field [54, 55].

2.5.1 Synthesis of Ag/TiO_2 for use in water treatment

Since bacteria are one of the factors contributing to water pollution, scientists have been trying to come up with ways and strategies of creating antibacterial agents. Silver nanomaterials and silver-titania nanocomposites can effectively inhibit bacterial growth [56]. Silver nanomaterials are mostly preferred because they are able to inhibit bacterial growth at low concentrations also; silver can be homogeneously distributed into titania nanomaterials.

Ansari and co-workers (2009) synthesized TiO_2 / Ag nanocomposites to a very high antibacterial activity. E. coli ATCC 25922 was used as a model microorganism for all inactivation studies. TiO_2-free silver nanoparticles sintered at 500° C showed bacterial inhibition only by 30 %. One sample loaded with silver was calcined at 300℃ and showed a high bacterial inhibition both under UV irradiation and without UV irradiation. This implies that growth delay of E. coli is due to the presence of silver nanoparticles and not due to TiO_2 nanoparticles [56]. On the contrary, the silver loaded sample sintered at 500℃ showed no antibacterial activity in the absence of UV irradiation. This was suggested to be due to the fact that at higher temperatures TiO_2 crystals grow, thereby covering silver nanoparticles and decrease their ability in bacteria inhibition. TiO_2/Ag nanocomposite calcined at a moderate temperature (300℃) is found to be more suitable for bacterial growth inhibition.

Jing and co-workers (2011) carried out a study to compare the effect of titania nanoparticles and titania nanotubes as bacterial agents. Anatase titania nanoparticles with a surface area as high as 587.8 m^2/g were synthesized by the sol-gel method. These nanoparticles were further treated under microwave and anatase titania nanotubes could be obtained. Both titania nanotubes and nanopartilces were examined for antibacterial activity against Escheria Coli in dark and under UV irradiation. The results showed that Nanomaterials displayed good antibacterial activity in dark due to their low inhibitory concentration and a large diameter of antibacterial circle [57]. However, the nanoparticles displayed higher antibacterial activities

under UV irradiation. The differences in antibacterial activities between titania nanoparticles and nanotubes was suggested to be due to changes of their microstructure.

Yin and co-workers (2003) synthesized large scale and size controlled silver nanoparticles under microwave irradiation using $AgNO_3$ as a dopant. Formaldehyde was used as a reducing agent and trisodium citrate was used as a stabilizer. These reagents were chosen because they can be easily removed through washing. Sample A1 and A3 were prepared by microwave and conventional heating respectively using the same amounts of chemical reagents. It was found that the sample prepared by microwave irradiation had an average particle size and size distribution twice as much as that of the sample prepared by conventional heating [56,58]. It was also discovered that microwave irradiation promotes crystal growth of silver particles.

Lee and co-workers prepared TiO_2/Ag nanoparticles by the sol-gel method and used sodium citrate tribasic dihydrate as a reduction agent. The impact of $AgNO_3$ on the properties of nano TiO_2–Ag composites was studied. It was found that the anatase phase of Ag / TiO_2 remained stable even at the increase of $AgNO_3$ amount. The crystallite size of TiO_2 nanoparticles was not significantly increased at the increase of $AgNO_3$ amount but the crystallite size of Ag nanoparticles was increased [59]. TiO_2 – Ag nanoparticles were spherical and had a narrow size distribution. It was deduced that the amount of $AgNO_3$ has no effect on the phase transformation of TiO_2 / Ag and on the crystallite size of TiO_2.

Li and co-workers loaded TiO_2 nanotube arrays with highly dispersed Ag nanoparticles through an ultrasound aided photochemical route. The loading was done at different $AgNO_3$ concentrations. The SEM results revealed that the Ag contents on the TiO_2 nanotube arrays increased with an increase in $AgNO_3$ content [60]. The XRD results showed that when the $AgNO_3$ content was low, the peak corresponding to metallic Ag at $2\theta = 38.1°$ was covered by the peak at 38.4° which corresponds to 38.4. When $AgNO_3$ was increased two additional peaks at 44° and 64° corresponding to silver could be observed. These results prove that the silver loading was successful.

Sun and co-workers prepared silver loaded TiO_2 by photochemical impregnation method which they characterized by several techniques. It could be seen from the TEM results that silver nanoparticles were unevenly distributed on TiO_2 surface and also silver covered only

by part of TiO_2 surface. The BET results revealed that the silver loading decreased the surface area of TiO_2. The surface area of TiO_2 was 10.47 m^2 / g before silver loading and decreased down to 9.50 m^2 / g after being loaded with silver. The mechanism of silver loaded TiO_2 revealed that deposited silver on TiO_2 surface acts as a site where electrons accumulate. The better separation between electrons and holes on the modified TiO_2 surface allowed more efficiency for the oxidation and reduction reactions [61].

Silver nanoparticles were successfully embedded on TiO_2 nanotubes by the polyol process. The as-prepared TiO_2 nanotubes were immersed in Ag^+ electrolyte for different durations (3, 7 and 11 hours). The resultant products were then annealed at different temperatures, 723 K (450° C) and 923 K (650° C). The results revealed that Ag nanoparticles were evenly distributed on the exterior mouth of amorphous TiO_2 nanotubes. After calcining at 723 K some silver nanoparticles were easily deposited on the surface of TiO_2 nanotubes and the anatase peak on the XRD pattern was more intense and narrower. This suggests that the high crystallinity of the anatase phase plays an important role in improving the bonding between Ag and TiO_2. At 923 K Ag nanoparticles were not completely formed. This was because the nanotube structure was destroyed by high temperatures and also the evolution of rutile may retard the formation of Ag nanoparticles [62].

TiO_2 nanotubes were prepared by electrochemical anodic oxidation and calcined at 450° C before loading with silver. Different concentrations of $AgNO_3$ were used to control the amount of silver loaded on TiO_2 nanotube arrays [63]. For Ag-TiO_2 nanotube arrays obtained in 0.002 M, 0.006 M, 0.010 M and 0.014 M $AgNO_3$ solution, the number of Ag nanoparticles on top of each nanotube is about 3, 5, 7 and 10 respectively. When $AgNO_3$ was at the concentration of 0.006 M Ag nanoparticles with the diameter of 10 – 15 nm were highly dispersed on the surface of the nanotubes. All the samples were crystallized into the anatase structure. When the concentration of Ag was below 0.01 M diffraction peaks corresponding to silver could not be seen due to low Ag content. But when the concentration was increased to 0.014 M peaks corresponding to silver emerged and this proved that silver loading into the nanotubes was successful [63].

L. Miao and his co-workers reported on the synthesis of titania nanotubes by hydrothermal treatment followed by calcination. Some of the formed nanotubes were loaded with silver

nanoparticles. The TEM results revealed that the tubes had an internal diameter of 7 nm and an outer diameter of 10 nm. Pure anatase tubes possessed a titanate structure while Ag loaded nanotubes possessed a TiO_2 structure with an anatase phase with an inner diameter of 5 - 7 nm and an outer diameter of 10 nm [64]. Silver nanoparticles had a sharp size distribution. About 80 % of silver nanoparticles were in a range of 1.7 to 3.5 nm.

2.6 Conclusion

Surface properties of TiO_2 can be controlled by employing different synthesis conditions, methods and different starting materials. In wet-chemical processing the sol-gel is the most favoured as it offers a number of advantages including excellent homogeneity and high purity materials. The hydrothermal treatment can yield nanomaterials with unique morphologies possessing large surface areas. Microwave assisted hydrothermal treatment can yield particles with uniform diameters, particle sizes and uniform distribution of particles. Energy delivery is very efficient because there is no heat transfer in microwave heating.

2.7 References

1. Yoshinagaa, M., Yamatoa, K., Satoa, N., Aokib, K., Morikawab, T., (2009) *Applied Catalysis B: Environmental:* Remarkably enhanced photocatalytic activity by nickel nanoparticle deposition on sulfur-doped titanium dioxide thin film 87, 239-244
2. Benabbou, A. K., Derriche, Z., Felix, C., Lejeuno, P., Guillard, C., (2007) *Applied Catalysis B: Environmental*, Photocatalytic inactivation of Escheria coli effect of concentration of TiO_2 and microorganism, nature and intensity of UV irradiation 76, 257-263
3. Charinpanitkul, T., Lorturn, P., Ratismith, W., Viriya-empikul, N., Tumcharern, G., Wilcox, J., (2011) *Materials Research Bulletin* : Hydrothermal synthesis of titanate nanoparticle/carbon nanotube hybridized material for dye sensitized solar cell application 46, 1604–1609
4. Qui, Y., and Yu. J., (2008) *Solid State Communications* : Synthesis of titanium dioxide nanotubes from electrospun fiber templates 148, 556-558
5. Mital, G. S., and Manoj, T., (2010) *Physical Chemistry* : A review of TiO_2 nanoparticles 56, 1639-1657

6. Sen, S., Mahanty, S., Roy, S., Heintz, O., Bourgeois, S., Chaumont, D., (2005) *Thin Solid Films* : Investigation on sol-gel synthesized Ag – doped TiO_2 cemert thin films 474, 245 -249
7. Diebold, U., (2003), *Surface Science Reports*: The surface science of titanium dioxide 48, 53–229
8. Garcia-Serrano, J., Gomez-Hernandez, E., Ocampo-Fernandez , M., Pal, U., (2009) *Current Applied Physics*: Effect of Ag doping on the crystallization and phase transition of TiO_2 nanoparticles, 9, 1097-1105 (TiO_2)
9. Hearne, G. R., Zhao, J., Dawe, A. M., Pischedda, V., Maaza, M., Nieuwoudt, M. K., Kibasomba, P., Nemraoui, O., and Comins, J. D., (2004), *Physical Review B*: Effect of grain size on structural transitions in anatase TiO_2: A Raman spectroscopy study at high pressure 70, 134102
10. Yodyingyong, S., Saekung, C., Panijpan, B., Triampo, W., Triampo, D., (2011) *Bull.Soc.Ethiop*: Physicochemical properties of nanoparticles titania from alcohol burner calcination 2, 263-272
11. Su, C., Hong, B, Y., Tseng, C. M., (2004) *Catalysis Today* : Sol – gel preparation and photocatalysis of titanium dioxide 96, 119 -126
12. Chen, J, P., and Lin, W. S., (2003) *Enzyme and Microbial Technology*: Sol-gel powders and supported sol-gel polymers for immobilization of lipase in ester synthesis, 32, 801-811
13. Shipeng, Q., and Kalita S. J., (2006) *Materials Science and Engineering A* : Synthesis, processing and characterization of nanocrystalline titanium dioxide 435, 327 - 332
14. Behnajady, M. A., Eskandarloo, H., Modirshahla, N., M. Shokri, M., (2011) *Journal of Desalination* : Investigation of the effect of sol-gel synthesis variables on structural and photocatalytic properties of TiO_2 nanoparticles 278,10 - 17
15. Tan, T. T. Y., Yip, C. K., Beydoun, D., Amal R., (2003) *Chemical Engineering Journal*: Effects of nano-Ag particles loading on TiO_2 photocatalytic reduction of selenate ions 95, 179 - 186
16. Wong, C. L., Tan, Y. N., Mohamed, A. R., (2011) *Journal of Environmental Management* : A review on the formation of titania ananotube photocatalysts by hydrothermal treatment 92, 1669-1680

17. Markowska, A., Szczupak, K., Ulfig, A., Morawski, W., (2011) *Catalysis Today*: The application n of titanium dioxide for deactivation of bioparticulates: An overview 169, 249-257
18. Jing Liqiang, J., Xiaojun, S., Weimin, C., Zili, X., Yaoguo, D., Honggang, F., (2003) *Journal of Physics and Chemistry of Solids* : The preparation and characterization of nanoparticle TiO_2/Ti films and their photocatalytic activity 64, 615–623
19. Wang, C. C., and Ying, J. Y., (1999) *Chem. Mater* : Sol-gel synthesis and hydrothermal processing of anatase and rutile titania nanocrystals, 11, 3113-3120
20. Zongbiao, G., Haigiang, W., Yueliu, W., Zuoliang, G., (2008) *Journal of Hazardous Materials:* Photocatalytic oxidation of nitric oxide with immobilized titanium dioxide films synthesized by hydrothermal method 151, 17-25
21. Wang, C., Deng, Z. X., Li, Y., (2001) *Inorg. Chem.* : The synthesis of nanocrystalline anatase and rutile titania in a mixed organic media 40, 5210-5214
22. Hou, Y., Zheng, H., Ding, Z., Wu, L., (2011) *Powder Technology* : Effects of sintering temperature on physicochemical properties and photocatalytic activity of titanate nanotubes modified with sulfuric acid, 214, 451 - 457
23. Ovenstone, J., and Yanagisawa, K., (1999) *Chem Mater* :Effect of hydrothermal treatment of amorphous titania on the phase change from anatase to rutile during calcination 11, 2770 - 2774
24. Yanagisawa, K., and Ovenstone, J., (1999), *J. Phys. Chem. B* : Crystallization of anatase from amorphous titania using the hydrothermal technique: effects of starting material and temperature 103, 7781-7787
25. Wu, X., Jiang, Q. Z., Ma. F. Z., Fu, M., Shangguan, W. F., (2005) *Solid State Communications* : Synthesis of titania nanotubes by microwave irradiation 136, 513 - 517
26. Kumar, S. R. Suresh, C., Vasudevan, A. K., Suja, N. R., Mukundan, P., Warrier K. G. K., (1999) *Materials Letters*: Phase transformation in sol-gel titania containing silica 38, 161 - 166
27. Qamar, M., Yoon, C. R., Oh, H. J., Lee, N. H., Park, K., Kim, D. H., Lee, K. S.,W. J., Lee, Kim, S. J., (2008) *Catalysis Today* : Preparation and photocatalytic activity of nanotubes obtained from titanium dioxide 131, 3 -14

28. Wilson, G. J., Matijasevich, A. S., Mitchell. D. R. G., Schulz, J. C., Will, G. D., (2006) *Langmuir* : Modification of TiO_2 for enhanced surface properties : finite Ostwald ripening by a microwave hydrothermal process 22, 2016 – 2027
29. Kasuga, T., Hiramatsu, M., Hoson, A., Sekino, T., Niihara, K., (1998), *Langmuir*: Formation of titanium oxide nanotubes 14, 3160-3163
30. Cui, L., Hui, K. N., Hui, K. S., Lee, S. K., Zhou, W., Wan, Z. P., Ha, C. N., (2012) *Materials Letters* : Facile microwave-assisted hydrothermal synthesis of TiO2 nanotubes 75, 175–178
31. Kasuga, T., (1999) *Advanced Materials* : Titania nanotubes prepared by chemical processing 11, 1307-1311
32. Wang, D., Yu, B., Zhou, F., Wang, C., Liu, W., (2009) *Materials Chemistry and Physics*: Synthesis and characterization of anatase TiO_2 nanotubes and their use in dye-sensitized solar cells 113, 602–606
33. Calabria, J., Vasconcelos, W. L., Daniel, D. J., Charter, R., Mcphail, D., Boccaccini, A. R., (2010) *Construction and Building Materials*: Synthesis of sol-gel titania bactericide coatings on adobe brick, 24, 384-389
34. Chen, Q., Zhou, W., Du. G., Peng, L. M., (2002) *Adv. Mater.* : Tritanate nanotubes made via a single alkali treatment 14,1208 -1211
35. Sikhwivhilu, L. M., Sinha-Ray, S., Coville, N. J., (2009) *Appl. Phys A*: Influence of bases on hydrothermal synthesis of titanate nanostructures 94 , 963-973
36. Yu, J., And Yu, H., (2006) *Materials Chemistry and Physics* : Facile synthesis and characterization of novel nanocomposites of titanate nanotubes and rutile nanocrystals 100, 507 -512
37. Borkar, S. A., and Dharwadkar, S. R., (2004) *Ceramics International* : Effect of microwave processing on polymorphic transformation of TiO_2 30 ,509 - 514
38. Wu, X., Jiang, Q. Z., Ma, Z. F., Fu, M., Shangguan, W. F., (2005) *Solid State Communications* : Synthesis of titania nanotubes by microwave irradiation 136, 513 - 517
39. Zhang, J., Wang, Y., Yang, J., Chen, J., Zhang, Z., (2006) *Materials Letters* : Microwave- assited synthesis of potassium titanate nanowires 60, 3015-3017
40. Peng, T., Zhao, D., Dai, K., Shi, W., Hirao, K., (2005) *ACS Publications*: Synthesis of Titanium Dioxide Nanoparticles with Mesoporous Anatase Wall and High Photocatalytic Activity 109, 4947-4952

41. Chen, Y. F., Lee, C. Y., Yeng, M. Y., Chiu, H. T., (2003) *Journal of Crystal Growth* : The effect of calcinations temperature on the crystallinity of TiO_2 nanopowders 247, 363 - 370

42. Sikhwivhilu, L. M., Mpelane, S., Mwakikunga, B. W., Sinha Ray, S., (2012) *Applied Materials and Interfaces* : Photoluminescence and hydrogen Gas-Sensing properties of titanium dioxide nanostructures synthesized by hydrothermal treatments 4, 1656 - 1665

43. Park, M. S., and Yoon, W. Y., (2003) *Journal of Power Sources* : Characteristics of a Li / MnO_2 battery using a lithium powder anode at high-rate discharge 114, 237-243

44. Sumerel, J, L., Yang, W., Kisailus, D., Weaver, J, C., Choi, J, H., Morse, D, E., (2003) *Chem. Mater* : Biocatalytically Templated Synthesis of Titanium Dioxide 15, 4804–4809

45. Khan, S. S., Mukherjee, A., Chandrasekaran, N., (2011) *Colloids and Surfaces A: Physicochem. Eng. Aspects* : Interaction of colloidal silver nanoparticles (SNPs) with exopolysaccharides (EPS) and its adsorption isotherms and kinetics : Article In Press

46. Bankar, A., Joshi, B., Kumar. A. R., Zinjarde, S., (2010) *Colloids and Surfaces A: Physicochem. Eng. Aspects* : Banana peel extract mediated novel route for the synthesis of silver nanoparticles 368 ,58–63

47. Yan, G., Chen, J., and Hua, Z., (2009) *Journal of Photochemistry and Photobiology A: Chemistry,* Roles of H_2O_2 and OH radical in bactericidal action of immobilized TiO_2 thin film reactor: An ESR study 207, 153-159

48. Rai, M., Yadav, A., Gade, A., (2009) *Biotechnology Advances* : Silver nanoparticles as a new generation of antimicrobials 27, 76–83

49. Sadeghi, B., Garmaroudi, F. S., Hashemi, M., Nezhad, H. R., Nasrollahi, A., Ardalan, S., Ardalan, S., (2010) *Advanced Powder Technology* : Comparison of the anti-bacterial activity on the nanosilver shapes: Nanoparticles, nanorods and nanoplates, Article in Press 23, (22 - 26)

50. Cao. H., Liu. X., Meng, F., Chu, P. K., (2011) *Biomaterials :* Biological actions of silver nanoparticles embedded in titanium controlled by micro-galvanic effects 32, 693 – 705

51. Seery, M. K., George, R., Floris, P., Pillai, S.C., (2007) *Journal of Photochemistry and Photobiology A*: *Chemistry* Silver doped titanium dioxide nanomaterials for enhanced visible light 189, 258-263

52. El-Nour, K. M. A., Eftaiha, A., Al-Warthan, A., Ammar, R. A., (2010) Arabian Journal of Chemistry 3, 135–140

53. Shahab, A. A., Mohammad, P., Azarmidokht, H., (2009) *Powder Technology:* Synthesis of TiO_2-Ag nanocomposite with sol-gel method and investigation of antibacterial activity against E.coli 196, 142-245

54. Noh, K. W., Woo, E., Shin, K., (2007) *Chemical Physics Letters* : Alteration of crystal structure of bismuth confined in cylindrical nanopores 444, 130–134

55. Mahendra, R., Alka, Y., Aniket, G., (2009) *Biotechnology Advances* Silver nanoparticles as a new generation of antimicrobials : 27, 76-83

56. Li-Yuan, C., Shun-wen, W., Beng, P., Zhu-ying, L., (2008) *Trans. Nonferrous Met. Soc. China* : Effect of thermal treating temperature on characteristics of silver doped titania 18, 980-985

57. Jing, Z., Guo, D., Wang, W., Zhang, S., Qi, W., Ling, B., (2011) *Solid State Sciences* : Comparative study of titania nanoparticles and nanotubes as antibacterial agents 13, 1797-1803

58. Yin, H., Yamamoto, T., Wada, Y., Yanagida, S., (2004) *Materials Chemistry and Physics* : Large-scale and size-controlled synthesis of silver nanoparticles under microwave irradiation 83, 66–70

59. Lee, M. S., Hong, S. S., Mohseni, M. D., (2005) *Journal of Molecular Catalysis A : Chemical* : Synthesis of photocalytic nanosized TiO_2 – Ag particles with sol-gel method using reduction agent 242,135 – 140

60. Li, J., Wang, C., Li, S., Lai, Y., H., Chen, H., Lin, C., (2009) *Journal of Hazardous Materials*: Ultrasound aided photochemical synthesis of Ag loaded TiO_2 nanotube arrays to enhance photocatalytic activity 171, 1045-1050

61. Liu, S. X., Qu, Z. P., Han, X. W., Sun, C. L., (2004) *Catalysis Today* : A mechanism for enhanced photocatalytic activity of silver-loaded titanium dioxide 93–95, 877–884

62. Liang, Y. Q., Cui, Z. D., Zhu, S. L., Liu, Y., Yang, X. J., (2011) *Journal of Catalysis* : Silver nanoparticles supported on TiO_2 nanotubes as active catalysts for ethanol oxidation 278, 276–287

63. Sun, L., Li, J., Wang, C., Li, S., Chen, Y. L. H., Lin, C., (2009) *Journal of Hazardous Materials* : Ultrasound aided photochemical synthesis of Ag loaded TiO_2 nanotube arrays to enhance photocatalytic activity171, 1045–1050

64. Miao, L., Ina, Y., Tanemura, S., Jiang, T., Tanemura, M., Kaneko, K., Toh, S., Mori, Y., (2007) *Surface Sciences*: Fabrication and photocromic study of titanate nanotubes loaded with silver nanoparticles 601, 2792 - 2799

CHAPTER 3

EXPERIMENTAL

3.1 Introduction

In this chapter the experimental procedures to achieve the outlined objectives are carried out. The procedures are outlined as follows: synthesis of titania nanostructures by the sol-gel method; morphological transformation of the aforementioned structures was performed by microwave assisted hydrothermal treatment; and post thermal treatment of the obtained products. Finally, all materials were characterized to determine the effect of these treatments.

3.2 Chemicals and reagents

The reagents used in this work were titanium tetraisopropoxide (TTP) which was obtained from Merck, potassium hydroxide, ethanol, methanol, 2-propanol, 1-butanol, 2-butanol, $AgNO_3$ and ammonium hydroxide also purchased from Merck chemicals.

3.3 Equipment

The following instruments were used to characterize all the prepared materials; Scanning electron microscope, transmission electron microscope, X-ray diffraction spectrometer, fourier transformer infrared spectrometer and Brunauer-Emmert-Teller surface analyser.

3.4 Method of synthesis of TiO_2

3.4.1 Sol-gel

The sol-gel method has been extensively used in recent years for the fabrication of nanomaterials [1].This method is defined as the chemical synthesis of oxides involving hydrolysable alkoxides that undergo a sol-gel transition. Sol-gel processing has been used to prepare glasses, glass-ceramics, and ceramics. Either amorphous or crystalline materials can result depending on the composition, the precursor, handling, and heat treatment [2]. The sol is a colloidal suspension of solid particles in a liquid. The ceramic materials are prepared in the sol-gel process through the following three stages: preparation of a sol, gelation of a sol and removal of a solvent [3] .The sol-gel process can be used to prepare materials in the nanometre scale that have ultrastructure control. During the sol-gel process a transition occurs, which involves many chemical and structural processes. The unique advantages of the sol-gel process, compared to other methods are: possibility of deposition onto complex-shaped

substrates, easy control of the doping level, relatively inexpensive starting materials and simple equipment [4, 5]. Through the sol-gel method compositional and microstructural tailoring of the products can be achieved by controlling the chemistry of the precursor and the processing conditions [6, 7]. This means that it can produce homogeneous and relatively high purity products. The precursors for synthesizing sols consist of a metal alkoxide or an inorganic salt surrounded by different reactive ligands. When using the metal organic route based on metal alkoxides in organic solvents the steps / processes take place. Inorganic step polymerization reactions take place through hydrolysis and condensation of metal alkoxides $M(OR)_Z$. Where M is an alkoxy group e.g. titanium and Z is the valence or oxidation state of the metal.

Step 1: hydrolysis of alkoxy group leading to hydroxylation.

$$M - OR + H_2O \longrightarrow M - OH + R - OH \qquad \text{(i)}$$

Step 2: Polycondesation process resulting in the formation of branched oligomers and polymers with a metal oxo-based skeleton and reactive residual hydroxo and alkoxy groups. This involves two mechanisms:

$$M - OH + HO - M \longrightarrow M - O - M + H_2O \qquad \text{(ii)}$$

Alcohol Condensation:

$$M - OH + RO - M \longrightarrow M - O - M + ROH \qquad \text{(iii)}$$

The hydrolysis reaction replaces alkoxide groups (OR) with hydroxyl groups (OH) through the addition of water. "Subsequent condensation reactions involving the M – OH groups produce M- O – M bond plus the water or alcohol by-products"[8]. In most cases condensation begins before the hydrolysis process is complete. In the sol-gel process alcohols are used as solvents because alkoxides and water are immiscible.

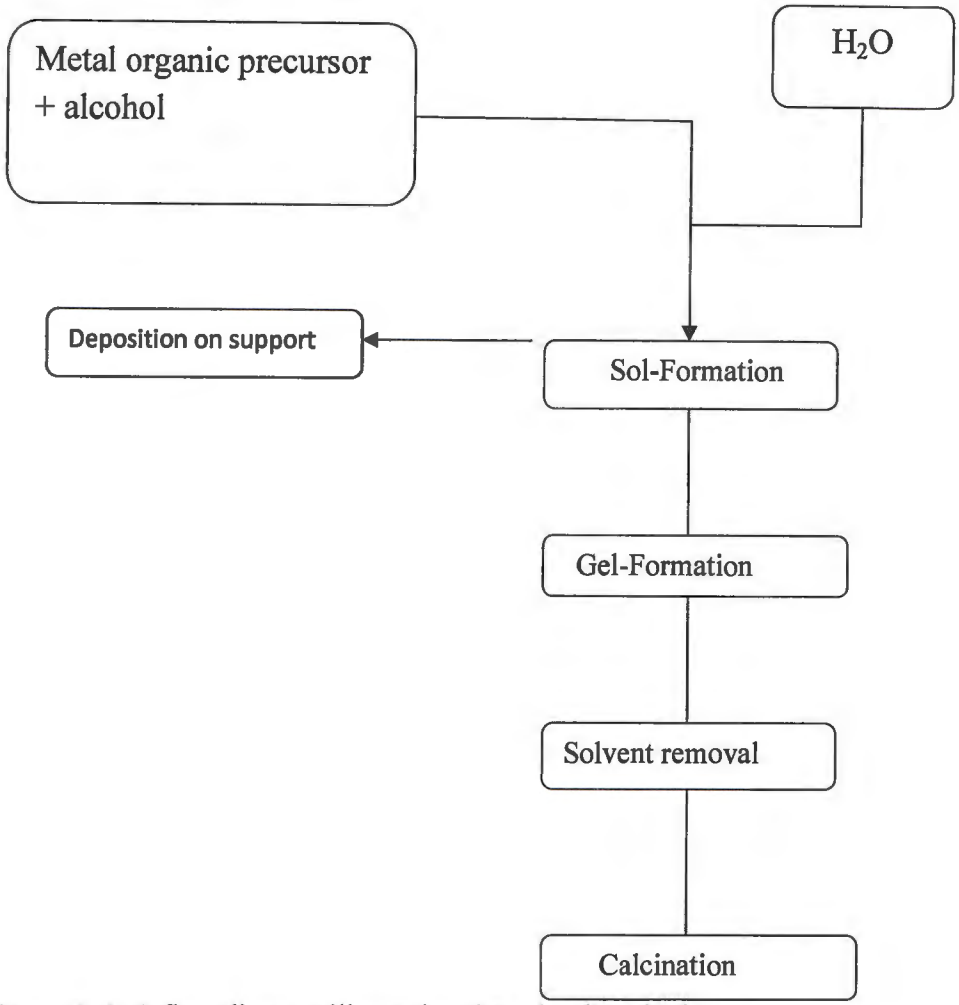

Figure 3. 1: A flow diagram illustrating the sol-gel method

3.5. Engineering of low dimensional systems

3.5.1 Conventional heating hydrothermal method

Methods such as the assisted-template method, the sol-gel, electrochemical anodic oxidation method and hydrothermal treatment are presently used for the production of TiO_2 nanotubes. Among these methods only the hydrothermal treatment can yield low dimensional, well separated, crystallized nanostructures and is suitable for large scale production. [9]. It is environmentally friendly because the reactions take place in an aqueous solution inside a closed vessel using water as a reaction medium. The hydrothermal method is a convenient method for the synthesis of low dimensional structures because it has advantages such as generation of highly crystalline structures, good control over crystal composition, usage fewer reagents thereby producing relatively purer materials. Though the reaction pathway is sensitive to experimental conditions such as pH, temperature, and treatment time, this

technique can yield cost-effective titania nanotubes in a simple manner under controlled conditions.

3.5.2 Microwave-assisted Hydrothermal Processing

Microwave synthesis is an ideal method for synthesizing one dimensional nanomaterials. This technique has the potential to fabricate nanomaterials with different morphologies such as nanotubes, nanorods, nanowires, nanospheres, etc. [10]. This technology is applicable in material science for process control, drying of ceramic sanitary ware, calcination, powder synthesis and sintering [11]. It can also be used to synthesize inorganic materials such as metallic nanostructures, metal oxides, zeolites and others. Crystal size and shape are important factors in nanoparticle research. Nonetheless, control of morphological properties and composition of a product has been a major challenge [12]. However, microwave processing offers an alternative approach towards solving these problems, [13, 12] Microwave processing is faster compared to the conventional heating method. This is because energy is delivered through direct interactions with the molecules and electromagnetic waves, so no heat is lost through conduction or convection. Therefore energy delivery is very efficient. There is no heat transfer in microwave heating; instead energy is converted from electromagnetic energy to thermal energy. This energy is able to penetrate the material and in this way energy can be generated throughout the entire volume of the material. Microwave energy can penetrate even thick materials because heat transfer does not rely on diffusion of surfaces. Therefore microwaves can save time and quality of the material [13].

An area of microwave processing that has received a lot of attention is ceramic processing. Ceramics have low thermal conductivities and are therefore processed at high temperatures. Most ceramic materials including silicon carbide (SiC) and magnesium oxide (MgO) have dielectric properties that are suitable for microwave processing. However, materials such as silicon nitride (Si_3N_4) and alumina (Al_2O_3) are poor absorbers of microwaves up to a critical temperature [14]. Above this temperature, the dielectric loss factor begins to increase and the material begins to form a link with microwaves [14]. Ceramics that must reach a critical temperature before they link with microwaves are difficult to process. Before reaching the critical temperature, these materials have very low loss factor and for this reason they get heated very slowly in the microwave field. Ceramic processing in non-uniform electromagnetic fields leads to the variation of local temperature within the material. If the

critical temperature is first reached within the local volume before the rest of the material, then that particular area will begin to heat very fast and the temperature will rise even more in the entire material. This can result in localized thermal runaway that can cause stresses that are high enough to fracture the material. However, materials that exhibit this behaviour can be processed by hybrid heating. During this process, the ceramic is heated through traditional heat transfer before the critical temperature is reached. As the material begins to get heated, and its loss factor increases it begins to couple more effectively with microwaves. In microwave processing the material is directly heated, therefore the thermal gradients due to convective and radiative heat loss from the surface of ceramic to the unheated cavity occur. To avoid steep reverse thermal gradients, the surface of the ceramic is often insulated from the unheated microwave cavity. Ceramics are particularly susceptible to thermal gradients because thermal stresses can be high enough to initiate fracture in brittle ceramics.
Energy is transferred to materials by interaction of the electromagnetic fields at the molecular level, and the dielectric properties ultimately determine the effect of the electromagnetic field on the material. Thus, the physics of the microwave / materials interaction is of primary importance in microwave processing. The interaction of microwaves with molecular dipoles results in rotation of the dipoles, and energy is dissipated as heat from internal resistance to rotation.

Microwave furnaces consist of three major componenets: the source, the transmission lines and the applicator. The microwave source generates the electromagnetic radiation and the transmission lines deliver the electromagnetic energy from the source to the applicator. In the applicator the energy is either absorbed or reflected by the material. The acceleration of reactions by microwave exposure results from material – wave interactions leading to thermal effects. Thermal effects can result from dipolar polarization as a consequence of dipole – dipole interactions between polar molecules and electromagnetic field. They originate in dissipation of energy into heat as an outcome of agitation and intermolecular friction of molecules when dipoles change their mutual orientation at each alternation of electrified at a very high frequency. This energy dissipation the core materials allow a much more regular repartition in temperature compared to conventional heating.

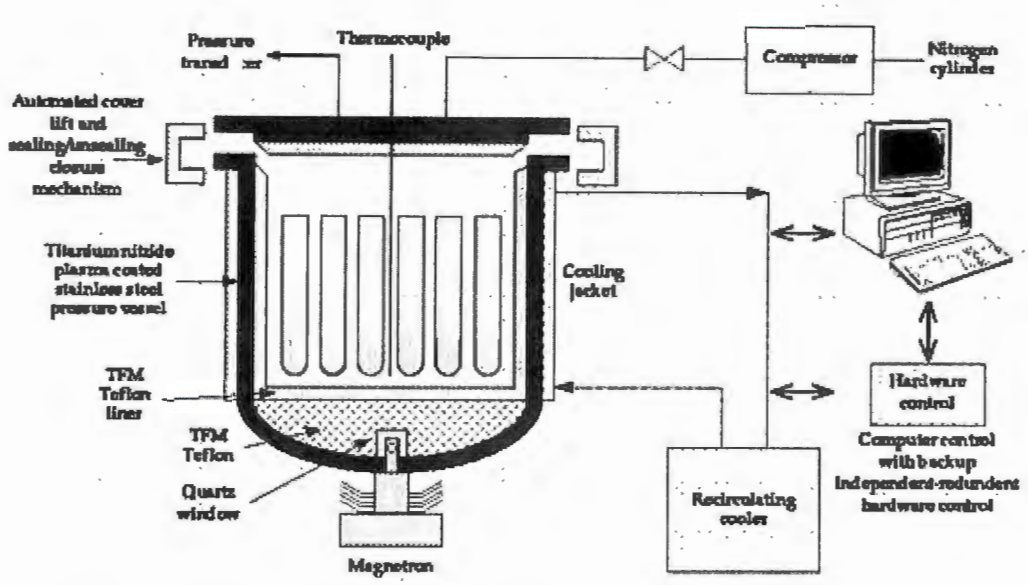

Figure 3.2 : A Schematic set-up illustrating the microwave assisted hydrothermal technique. [15]

3.5.3 Electrochemical anodic oxidation method

Anodic oxidation is a method used to prepare highly ordered TiO_2 nanotube arrays on Ti substrate [16]. It has been a traditional surface modification method to modify the structures and chemical properties of anodic films on titanium. Controlling the electrochemical parameters such as electrolyte composition and concentration, applied potential or current and temperatures monitors this. In recent times anodic oxidation has become an attractive method for preparing oxide films on titanium because the oxide films improved apatite in SBF (simulated body fluids) [17]. This method is also applied industrially to synthesize films, ceramics and powders. It can also be utilized for the treatment of waste waters. In the electrochemical synthesis of ceramics by the anodic method, a metal ion or complex is oxidized at the electrode surface. The pH of the solution is adjusted so that the initial oxidation state is stable, but the higher oxidation state readily undergoes hydrolysis to a metal hydroxide or oxide

3.5.4. Microemulsion method

Microemulsion methods consist of large amounts of two immiscible liquids for instance, oil and water that are brought together into a single phase [18]. They are usually optically clear, thermodynamically stable and are low viscous solutions. They have the capacity to solubilize both aqueous and oil soluble compounds. These techniques can be utilized in a variety of chemical and industrial process. They can be applied in detergency, cosmetics, agrochemicals, food, pharmaceuticals, analytical applications, nanoparticle synthesis and many others [19].

3.6 Composites

A composite can be defined as a combination of two or more different materials made to blend the best properties of both [20]. Nanocomposites can be ceramic, metallic, metal oxides, polymer based, metal-metal (alloy), metal-metal oxide, and organic materials. They can be compact bulk materials, thin films or mesoporous host – guest performs [21]. In nanocomposites, one of the components must have at least one dimension in a nanoscopic range, which is around 10^{-9}m. In the engineering of materials, most materials do not have all the necessary properties suitable for certain applications. However, these properties can be improved by addition of other materials. This may result in the development of totally new properties that do not exist in either of the constituents. Composites are produced by simultaneous precipitation of the core and coating materials. This leads to a dispersion of particles of the core materials into the matrix of a coating material. They can also be formed by particles of pure coating materials first and then impregnate with the active components. Such formulations possess advantages including achieving a controlled delivery of the active ingredient into its targeted media. When a composite is being designed it is important to alter the properties of the materials in order to suit the desired performance across various length scales [21]. Surface area to volume ratio of the reinforcement material is an important characteristic in the understanding of the structure property relationship of nanocomposites.

3.7 Methods of loading

There are various strategies used to introduce the active phase on the surface of an inert support. This is done to minimize the amount of the active phase and to control both the size and size distribution of this active phase whilst promoting good dispersion. These strategies include incipient wetness, co-preciptation, deposition precipitation, etc.

3.7.1 Wet Impregnation method

This method entails preparation of composite materials whereby the matrix is generated from a solid support material and an aqueous metal solution [22]. In this technique the nanotube surface is impregnated with a solution of the metal precursor salt followed by drying, calcinations and reduction to yield metal particles anchored on the nanotube surface [23]. Wet–impregnation method is the most commonly used because it is simple and cost – effective. It is mostly used in the catalyst industry to impregnate metals in the pore of a support medium [22]. This method can also be used for chemical looping oxygen carrier synthesis. This method can also be used to chemical looping oxygen carrier synthesis, which is a technique that involves the use of an oxygen carrier that transfers oxygen from the air to the fuel. The oxygen carrier is composed of a metal oxide as an oxygen source, and an inert as a binder for increasing the mechanical strength of the carrier

3.7.2 Co-precipitation method

The process of co-precipitation involves precipitating multi-compound system in a matrix. Solid precipitates are formed and are filtered to obtain a homogeneous matrix formation [24]. This method is applied in less porous materials. Its preparation route involves the use of three precursors as follows; the metal salt solution, the support solution and the precipitating agent [25]. A co-precipitation agent is formed by a solution of inorganic or organic salt. The main parameters in this method are pH, temperature, concentration and mixing rate. However, these parameters need to be regulated carefully. Though effective, this method suffers from several disadvantages including: lengthy and time consuming separations, the analytical solution after preconcentration contains a high level of carrier precipitate which can give rise to non-specific scatter and matrix interferences in the flame of the atomic absorption instrument [24].

3.8 Characterization

Bulk materials differ in physical and chemical properties from their smaller forms. The smaller forms can be in micrometer, nanometer. Materials need to be characterized in order to determine their different properties such as electrical, optical, magnetic, mechanical, and structural. A change in form, size or shape of the material can change the structural or chemical property of a material. For the reason that materials differ in properties, different characterization tools are employed in every case. These tools are classified in different ways

depending on the kind of property (electrical, optical or mechanical) to be characterized [25]. In this study characterizations of samples were carried out using different techniques such as X-ray Diffraction, Transmission Electron Microscopy, Scanning Electron Microscopy, B Brunauer-Emmet-Teller method and Fourier- Transform Infrared Spectrometer.

3.8.1 X-ray Diffraction

X-ray methods provide information on material and nanoparticle structure, particle size and information [26]. X-ray spectrometry is a non-destructive and multi-elemental technique widely used for elemental analysis [27]. Thus, it can be used to provide crystal size, degree of crystal disorder as well as various crystal structure characteristics. The crystallite size can be calculated using the Debye-Scherrer equation:

$$d = \frac{K\lambda}{\beta \cos\theta} \qquad \text{(i)}$$

where K is the shape factor and has a value of about 0.9, λ is the x-ray wavelenghth, β is the line broadening at half the maximum intensity (FWHM) in radians, and θ is the Bragg angle and d is the crystallite size. The Scherrer equation is limited to nano-scale particles. It is not applicable to grains larger than about 0.1 μm. The XRD method offers a number of significant advantages over other methods. It is rapid and fairly affordable [28]. The basic XRD system consists of an x-ray generator, a device to hold and rotate the sample and a detector. During the analysis of elements diffraction occurs. As a result x-rays get scattered and interference between the waves scattered by these x-rays occurs. It is in fact atomic planes which reflect and diffract x-rays. The diffracted rays interfere with each other such that when their path difference is an integral multiple of the wavelength, the interference is constructive otherwise it is destructive. This is the principle on which Bragg's law is based. Hence we have a diffracted radiation that has the power that depends on the direction of observation. The diffraction pattern of a crystalline material records the x-ray intensity as a function of the scattering angle and it offers a clue to the crystal structure. Because the atoms form a regular array, the diffracted waves can reinforce at certain diffraction angles and cancel each other at all other angles. Thus, interference peaks are formed at these angles [26]. Any crystalline material immersed in a white x-ray beam diffracts along given directions, according to Bragg's law:

$$2d_{(hk)}\sin\theta_B = \lambda \qquad \text{(ii)}$$

where d_{hk} is the interplanar spacing of (hkl) crystallographic planes, θ_B is the Bragg angle and λ is the wavelength of the incident beam. Figure 3.2 is an experimental setup that explains what happens during an X-ray analysis. The incident beam (λ = 1.38 A °) hit the long side of the sample which is perpendicular to the pole axes at an incident angle of α_i = 0.3. The scattered X-rays were detected with a two-dimensional area detector [29].

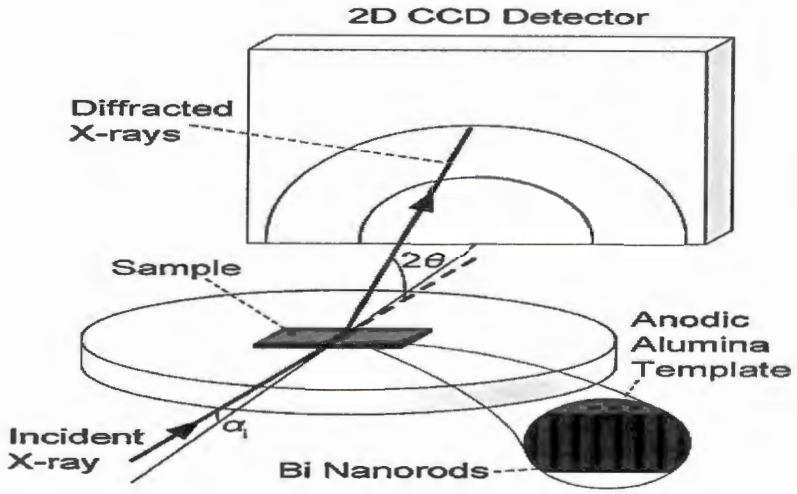

Figure 3.3 a schematic diagram of an X-ray diffraction spectroscopy [29].

3.8.2 Transmission Electron Microscope

In contrast to a SEM image, the TEM image contains three-dimensional information from the thin section of the sample [30]. This instrument can be used to analyze and provide structural information of metal oxides. It is also important for use in the analysis of thin film [31]. The most important application of TEM is the atomic resolution real-space imaging of nanoparticles. By forming nanometer size electron probe, TEM can identify the chemical and electronic structure of nanocrystals. In situ TEM is demonstrated for characterizing and measuring the thermodynamic, electric and mechanical properties of individual structures [32]. TEM instrument is very important as it can be used in most fields of research for characterization. A simple schematic representation of a transmission electron microscope is given in (Figure. 3.2). The electron gun is mounted at the top of the microscope column. During the analysis, the electron beam is focussed on the electromagnetic lenses. Transmitted electrons are projected onto a viewing screen or a photographic or electronic image recording device [33]. A high vacuum has to be maintained in the microscope column because electrons

are easily deflected. Only thin samples can be studied because electrons have a reduced penetration of matter. Heavy metals like lead, uranium and platinum are often used to improve the contrast because they can strongly interact with the electrons. The resolution in the TEM is directly proportional to the acceleration voltage of the electrons: with increasing voltage the wavelength of the electrons decreases resulting in higher resolution. Additionally, the contrast becomes poorer with increasing acceleration voltage as the scattering of the electrons is inversely proportional to their velocity [33].

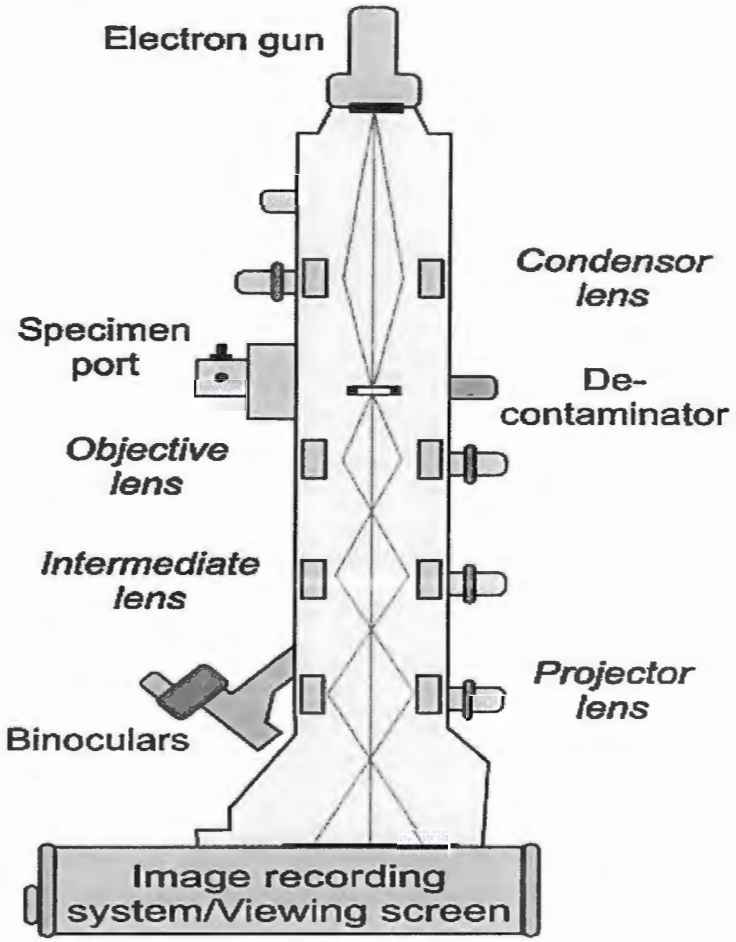

Figure. 3.4 A schematic representation of Transmission Electron Microscopy [33]

3.8.3 Fourier- Transform Infrared Spectrometers

Fourier transform Infrared Spectroscopy is a technique that is used in the laboratory to analyze materials [34]. It is used for identification of unknown materials, determination of the quality or consistency of the sample as well as determination of the amount of components in a mixture. An infrared spectrum represents a fingerprint of a sample with absorption peaks,

which correspond to the frequencies of vibrations between the bonds of the atoms making up the material. No two compounds can produce the exact same infrared spectrum because each material is a unique combination of atoms. Consequently, infrared spectroscopy can result in a positive identification of every different kind of material. Also, the size of peaks is a direct indication of the amount of material present. The mechanism of operation of FTIR is illustrated by figure 3 below. Infrared energy is emitted from a glowing black-body source. This beam passes through an aperture which controls the amount of energy presented to the sample (and, ultimately, to the detector). Then the beam enters the interferometer where the "spectral encoding" takes place. The resulting interferogram signal then exits the interferometer. The beam enters the sample compartment where it is transmitted through or reflected off the surface of the sample, depending on the type of analysis being accomplished. This is where specific frequencies of energy, which are uniquely characteristic of the sample, are absorbed. Finally, the beam passes to the detector for final measurement. The detectors used are specially designed to measure the special interferogram signal. The measured signal is digitized and sent to the computer where the Fourier transformation takes place. The final infrared spectrum is then presented to the user for interpretation and any further manipulation [35].

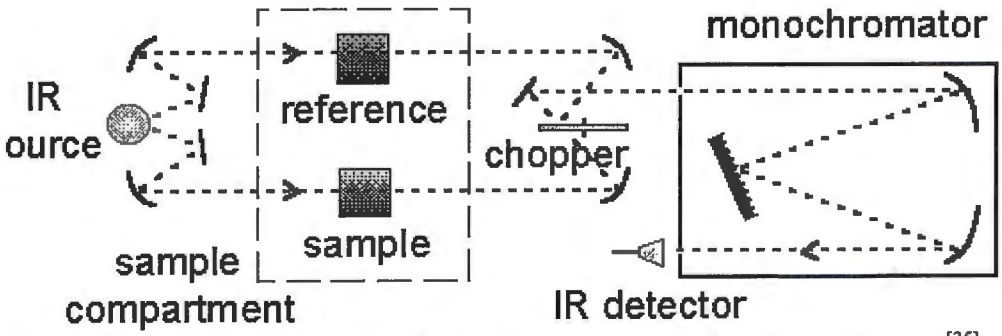

Figure 3.5 a schematic diagram of a Fourier Transform Infrared spectroscopy [35]

3.8.4 Brunauer-Emmet-Teller method

The specific surface area of a powder is determined by physical adsorption of a gas on the surface of a solid and by calculating the amount of adsorbate gas that corresponds to a monomolecular layer on the surface [36]. Physical adsorption occurs as a result of Van der Waals forces that are between the adsorbate gas molecules and the adsorbant surface of the test powder. The surface area is usually determined at the temperature of liquid nitrogen. The amount of a gas can be measured by a volumetric or continuous flow procedure. Before

determining the specific surface area of the sample, gases and vapours that may have been physically adsorbed during and after synthesis should be removed. This procedure is necessary; otherwise the specific surface area may be reduced or may be variable because an intermediate area of the surface is converted with molecules of the previously adsorbed gases or vapors. The out gassing conditions are critical and must be demonstrated to yield reproducible BET plots. The results should give a constant weight of test powder without any detectable physical or chemical changes in the test powder. The out gassing conditions such as temperature, pressure and time should be such that the nature of the solid surface does not change. Out gassing of many substances is usually carried out by either applying a vacuum or by a desorption-adsorption cycling method. In both cases high temperatures are applied to fasten the rate at which contaminants leave the surface.

The data are treated according to the Brunauer-Emmet and Teller (BET) adsorption isotherm equation:

$$\frac{1}{\left[Va\left(\frac{P_O}{P}\right)-1\right]}=\frac{C-1}{VmC}\times\frac{P}{P_O}+\frac{1}{VmC} \qquad \text{(iii)}$$

P is partial vapour pressure of adsorbate gas in equilibrium with the surface at 77.4 K (b.p of liquid nitrogen) in Pa. Po = Saturated pressure of adsorbate gas in Pa. Va is a Volume of gas adsorbed at standard temperature and pressure (STP) [273.15 K] and atmospheric pressure (1.013×10^5 Pa) in mL. Vm is a volume of gas adsorbed at STP to produce an apparent monolayer on the sample surface in mL. C is a dimensionless constant that is related to the enthalpy of adsorption of the adsorbate gas on the powder sample.

A value of Va is measured at each if not three values of P/Po

The BET value:

$$\frac{1}{\left[Va\left(\frac{Po}{P}-1\right)\right]} \qquad \text{(iv)}$$

Is plotted against P/Po according to equation (v). This plot should yield a straight line.

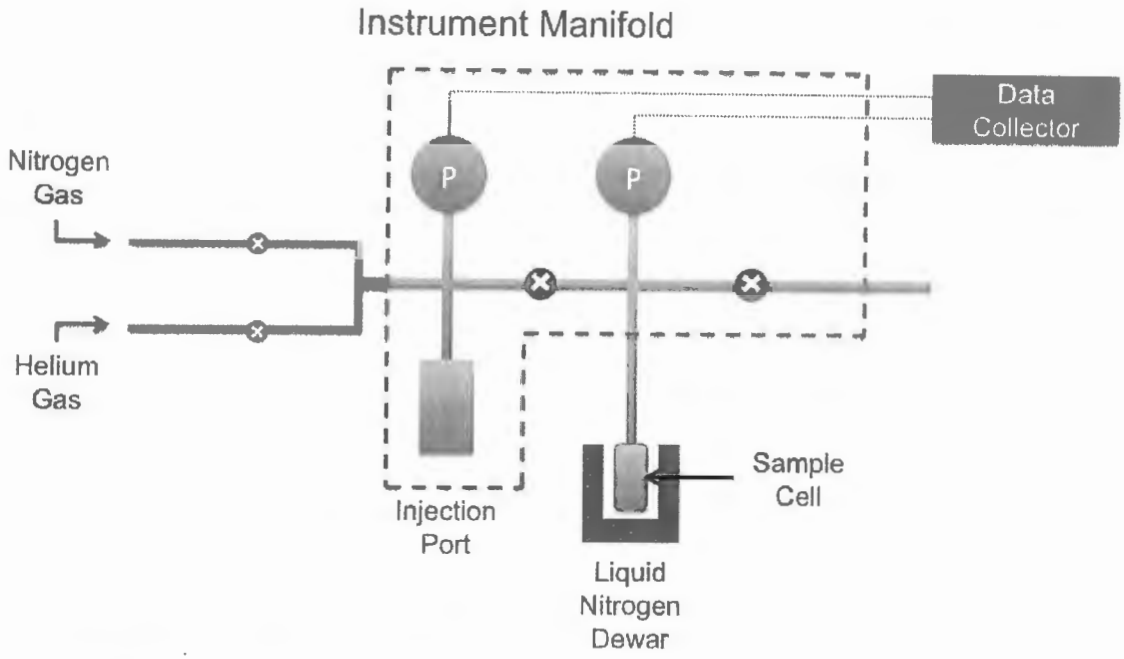

Figure 3.6 a schematic diagram of a Brunauer–Emmet-Teller [37]

3.8.5 Scanning Electron Microscope

The scanning electron microscope (SEM) permits the observation and characterization of heterogeneous organic and inorganic materials on a nanometer to micrometer scale. The major use of this technique is to obtain topographic images in the magnification range of 10 to 10 000 times. The major reason for the SEM's usefulness is the high resolution which can be obtained when bulk objects are examined. It has a large depth of field which is partly responsible for the three-dimensional appearance of the specimen. The greater depth also provides much more information about the specimen. The SEM is capable of examining objects at very low magnification. This feature is useful in many fields because it enables the SEM image to complement information from the optical microscope. In the SEM the area to be examined is irradiated with a finely focused electron beam. The types of signals produced from the interaction of the electrons with samples include secondary electrons, backscattered electrons, characteristic x-rays and other photons of various energies [38]. The signals are obtained from specific volumes within the sample and can be used to examine the characteristics of the sample. Thus the SEM offers many features that are very important in the study of samples in metallic and non-metallic systems. The unique advantages of the SEM include direct examination, a wide range of magnifications, minimal or no sample

preparation, a low specimen current and sufficient resolution [28]. The SEM consists of a lens system for focusing the electron beam, deflection coils for scanning, and a detector that collects secondary electrons emitted from the specimen. A schematic diagram is shown in Figure. 3.4. The electron beam is focused by a series of electromagnetic lenses, the condenser lenses (CL), and the objective lens (OL),and the beam-path is deflected by the deflector coils, allowing raster scanning using sequential trigonometric waveforms in the x-axis and waveform stepping in the y-axis. Usually, SEM resolution relies on well matched CL and OL for electron beam focusing. More importantly, however, an extremely high-resolution image requires a well-formed deflector coil current in the x- and y-axis, a low noise circuit, and additional devices including a stigmator for reducing image distortion. The scanning wave form must be adjusted considering the actual deflector coil current or voltage, which determines the scanning area of the specimen. The deflector is composed of a signal generator that produces a programmable scanning waveform, a driver for amplifying the signal and powering the coil, and scanning coils in the x- and y-axis. The scanning wave frequency and shape must be determined taking into consideration the impedance of the coils and the driver.

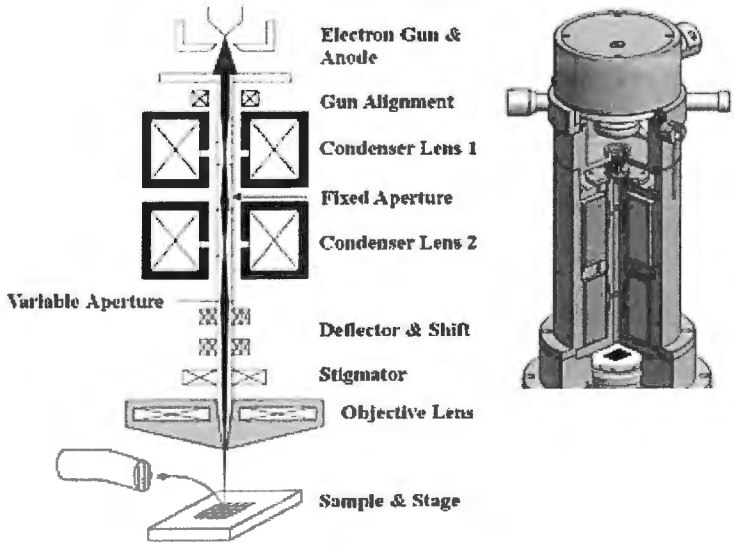

Figure 3.7 a schematic diagram of a scanning electron microscope [39]

3.9 References

1. Chen, X., and Schlueseher, H. J., (2008) *Toxicology Letters:* Nanosilver: A nanoproduct in medical application 176, 1-12
2. Brinker, C. J., and Scherrer, G. W., (1990) Sol-gel science : The physics and chemistry of sol-gel processing
3. Calabria, J., Vasconcelos, W. L., Daniel, D. J., Charter, R. J, Mcphail, D., Boccaccini, A. R., (2010) *Construction and Building Materials*: Synthesis of sol-gel titania bactericide coatings on adobe brick, 24, 384-389
4. Chen J. P., and Lin, W. S., (2003) *Enzyme and Microbial Technology*: Sol-gel powders and supported sol-gel polymers for immobilization of lipase in ester synthesis, 32, 801-811
5. Sen, S., Mahanty, S., Roy, S., Heintz, O., Bourgeois, S., Chaumont, D., (2005) *Thin Solid Films* : Investigation on sol-gel synthesized Ag – doped TiO_2 cemert thin films 474 , 245 -249
6. Wang, C. C., and Ying, J. Y., (1999) *Chem. Mater* : Sol-gel synthesis and hydrothermal processing of anatase and rutile titania nanocrystals, 11, (3113-3120)
7. Su, C., Hong, B.Y., and Tseng, C. M., (2004) *Catalysis Today* : Sol-gel preparation and photocatalysis of titanium dioxide 96, 119-126
8. Rondinini, S., Ardizzone, S., Cappelletti, G., Minguzzi, A., and Vertova, A., (2009) *Materials*: Sol-Gel synthesis, The University of Milan, Milan, Italy (614 - 624)
9. Ou, H., – H., and Lo, S., – L., (2007) *Separation and Purification Technology*: Review of titania nanotubes synthesized via hydrothermal treatment :Fabrication, modification and application 58, 179-191
10. Thostenson, E., T., and Chou, T., –W., (1999) *Composites*: Part A: Microwave Processing: Fundamentals and applications 30 ,1055-1071
11. Oghbaei, M., and Mirzae, O., (2010) *Journal of Alloys and Compounds* : Microwave versus conventional sintering : A review of fundamentals 494, 175-189
12. Bilecka, I., and Niederberger, M., (2010) Microwave chemistry for inorganic nanomaterials synthesis 2, 1358-1374
13. Zongbiao, G., Haigiang, W., Yueliu W., and Zuoliang, G., (2008) *Journal of Hazardous* : *Materials* Photocatalytic oxidation of nitric oxide with immobilized titanium dioxide films synthesized by hydrothermal method 151, 17-25

14. DeMille. D., Glenn. D. R., and Patricka. J., (2004) *The European Physical Journal D*: Microwave traps for cold polar molecules 31, 375 - 384
15. Kingston. H. M., Walter. P. J., (1998) Department of Chemistry and Biochemistry Duquesne University, Pittsburgh PA 15282 - 1503
16. Cui, X., Kim, H., Kawashita, M., Wang, L., Xiong, T., Kokubo, T., Namakura, T., (2009) *Dental Materials:* Preparation of bioactive titania films on titanium metal via anodic oxidation 25, 80-86
17. Kuromoto, N. K., Simao, R. S., and Soares, G. A., (2007) *Materials Characterization*: Titanium oxide films produced on commercially pure titanium by anodic oxidation with different voltages 58, 114-121
18. Zhang, W. J., He, Y. Q., and Qi, Q., (2005) *Materials Chemistry and Physics:* Synthesis of porous TiO_2 thin film of photocatalyst by charged microemulsion; 93 508-515
19. Li, G. L., and Wang, G. H., (1999) *Nanostructured materials:* Synthesis of nanometer-sized TiO_2 particles by a microemulsion method 11 663-668.
20. Thostenson, T. E., Ren, Z., Chou, T. W., (2001) *Composites Science and Technology*: Advances in the science and technology of carbon nanotubes and their composites: a review 61 1899-1912
21. Savage, N., Diallo, M., Duncan, J., Street, A., Sustich, R., (2009) Nanotechnology applications for clean water, *William Andrew Inc.* 49
22. Merhari, L., (2009) *Springer*: Hybrid nanocomposites for nanotechnology
23. Monhioux, M., (2012) Meta-nanotubes synthesis, properties and applications, *John Wiley and sons*
24. Fan, L. S., (2010) Chemical looping systems for fossil energy conversions, *John Wiley and sons*
25. Yan, G., Chen, J., Hua, Z., (2009) *Journal of Photochemistry and Photobiology A: Chemistry:* Roles of H_2O_2 and OH radical in bactericidal action of immobilized TiO_2 thin film reactor: An ESR study 207 (2-3) 153-159
26. Gladyszewski, G., Labat, S., Gergaud, P., Thomas, O., (1998) *Thin Solid Films*: Structure characterization of metallic layers by symmetric and asymmetric x-ray diffraction319, 78-80

27. Barroso, R. C., Anjos, J., Lopes, R. T., de Jesus, O., Braz, D., Castro, C. R., Uhl, A., (2002) *Radiation Physics* : Analysis of matrix characterization by x-ray diffraction and synchrotron radiation 65, 501-505

28. Last, W. M., Smol, J. P., Birks, H. B.,(2001) Tracking environmental change using lake sediments : Physical and geochemical; 2nd edition 153

29. Noh, K. W., Woo, E., Shin, K., (2007) *Chemical Physics Letters* : Alteration of crystal structure of bismuth confined in cylindrical nanopores 444 (130–134)

30. Skoog, D. A., Holler, F. J., Nieman, T. A., (1980) Principles of instrumental analysis, 5th edition, Philadelphia, Pa: Saunders College

31. Nakahara, S., (2003) Recent development in TEM specimen preparation technique using FIB for semiconductor devices; *Surface and coatings: Technology*, 169-170, 721-727

32. Wang, Z. L., (2000) *Journal of Physics and Chemistry:* Transmission electron microscopy of shape controlled nanocrystals and their assemblies; *B* 104 (6) 1153-1175

33. Kuntschea, J., Horst, J. C., Bunjes, H., (2011) *International Journal of Pharmaceutics*: Cryogenic transmission electron microscopy (cryo-TEM) for studying the morphology of colloidal drug delivery systems : Article In Press

34. Skoog, D. A., West, D. M., Holler, F. J., Fundamentals of Analytical Chemistry; Seventh Edition 557-595

35. Thermo Nicolet Corporation (2001) Introduction to Fourier Transform Infrared Spectrometry

36. Gelb, L. D., Gubbins, K. E., (1998) *Langmuir* : Characterization of porous glasses: Simulation models, adsorption isotherms and Brunauer – Emmett – Teller analysis method 14 2097-2111

37. Hwang, N.; Barron, A., (2011) BET Surface Area Analysis of Nanoparticles, Connexions Web site.http://cnx.org/content/m38278/1.1/

38. Goldstein, J., Newbury, D. E., Joy, D. C., Echlin, P. Lyman, C. E., Lifshin, E., (2003) Scanning electron microscopy and X-ray microanalysis; 3rd edition,

39. Kim, D. H., Kim, S. J., Oh, S. K., (2010) *Nuclear Instruments and Methods in Physics Research A* : Image improvement with modified scanning waves and noise reduction in a scanning electron microscope 620 112–120

CHAPTER 4

The effects of bio-alcohols on the Sol–gel prepared TiO_2 materials

4.1 Introduction

Different variables including time, temperature, doping and pH have been used to improve the properties of TiO_2 nanostructures. Nanosized TiO_2 materials with high surface areas have generated an increased interest because they possess unique optical, electrical and catalytic properties. Among many methods, sol-gel is one of the most used and preferred in the preparation of titanium dioxide nanostructures [1]. The sol-gel process can yield unique structures by controlling the starting material and processing conditions. This technique is known to yield products of high purity and excellent homogeneity [2]. In this chapter TiO_2 was synthesized using Titanium tetraisopropoxide (TTP) in the presence of bioalcohol (Methanol, ethanol, or butanol) or an inorganic base (NH_4OH). The objective was to evaluate the influence of nature and type of bio-alcohol on morphology, particle size and size distribution, and surface areas of TiO_2 derived nanostructures.

4.2 Experimental

4.2.1 Synthesis of TiO_2 nanostructures

TiO_2 was synthesized by mixing titanium isopropoxide (TTP) with one of four solvents at a time. The solvents were methanol, ethanol, 1-butanol, and ammonium hydroxide. That is, four products were obtained. A volume of 29.2 cm^3 of TTP was added drop-wise to 497.6 cm^3 of bio-alcohol with stirring (using a stirring rod). The mixture was then magnetically stirred for an hour and then aged in a glove box for 24 hours. A 263.46 cm^3 volume of the mixture was hydrolyzed with 18.02 cm^3 of deionized water. The solution was subjected to magnetic stirring for one hour and then placed in a glove box for 24 hours. The resultant solution was dried in an oven for 12 hours. The final product was obtained in powder form and was characterized by XRD, SEM, FT-IR, UV-vis, and BET. Table 4.1 below summarizes the process carried out during sample preparation prior to characterization.

Table 4.1: Preparation of xerogel material by reacting with various solvents

Designation	TTP / cm^3	Solvent name	Vol. of solvent / cm^3
SG 1	29.2	Methanol	497.6
SG 2	29.2	Ethanol	497.6
SG3	29.2	1-butanol	497.6
SG4	29.2	NH_4OH	497.6

4.2.2 Characterization of materials

In this study characterization of samples was carried out using different techniques. Scanning electron microscopy (SEM) was used to study the morphologies of the formed materials and the images were recorded using the AURIGA (Cross–Beam FIB SEM) operated at a voltage of 3 kV. The samples were first placed on a carbon tape and then sputter coated in K950 X (TURBO CARBON EVAPORATOR). The size, size distribution and shape of the structures were determined by transmission electron microscopy (JEOL JEM–2100 electron microscope). The samples were prepared by immersing the solid sample in ethanol and then subjected to ultrasonic treatment. For analysis, the samples were placed on a copper grid coated with a carbon film. The X-ray Diffraction was used to determine the crystallinity of the materials. The patterns were obtained from PANanalytical X'Pert PRO PW 3040/60 x-ray diffractometer Cu K_α = 0.154 nm monochromated radiation source, operating at 45.0 kV and 40.0 mA. XRD data were collected in the 2θ angle ranging from 1 to 90° with a step size of 0.02°. The specific surface area and the pore volume of the nanostructures were determined using the Brunauer-Emmet-Teller (BET) method. Before analysis the samples were degassed at 90 ° C in a vacuum for overnight. The transmittance spectra of the samples were collected from Spectrum 1000 FT-IR spectrometer (Perkin Elmer Precisely) at room temperature from 500 to 4500 cm^{-1}.

4.3 Results

4.3.1 BET

Table 4.2 presents the surface areas of materials prepared by the sol-gel method. The surface areas were determined using the Brunauer Emmet Teller method. 2.00 mg of the samples were first weighed. The samples were then degassed at 90° C to remove the moisture in the samples. Samples were then run in an instrument until analysis was complete. After this

procedure necessary calculations were done to obtain the final surface area. The results revealed that materials prepared in the presence of bioalcohols (aprotic organic solvents) possess the largest surface areas as compared to materials prepared in the presence of a weak inorganic base, NH_4OH (a protic inorganic solvent).

Table 4.2 BET surface areas of xerogel materials prepared by the sol-gel method.

Name	Description	Surface Area
SG 1	xerogel / methanol	398 m^2 / g
SG 2	xerogel / ethanol	413 m^2 / g
SG 3	xerogel / 1-butanol	388 m^2 / g
SG 4	xerogel / NH_4OH	369 m^2 / g

The surface areas of materials prepared in the presence of bioalcohols showed an interesting pattern shown in the graph below (Fig. 4.1). Materials prepared in the presence of methanol (bioacohol with one carbon) gave a surface area of 398 m^2 / g. When the chain length was increased to two carbons, the surface area was reasonably increased but when the chain length was increased even further to four carbons the surface area dropped. This suggests that the surface area had reached its maximum point when the alcohol with two carbons was used hence it dropped when the chain was increased further.

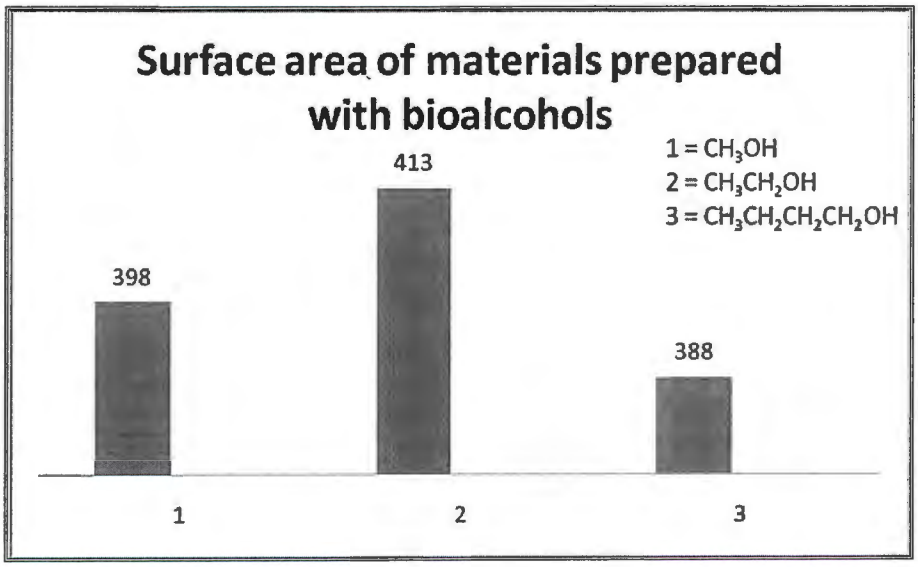

Figure 4.1 A graphical representation of surface areas of xerogel materials prepared with bio-alcohols.

4.3.2XRD

The XRD patterns of materials prepared by the sol-gel method are shown in figure (4.2). All the patterns showed a few broad peaks with little intensity. However, the peaks could not be indexed to any known material suggesting that the obtained materials are amorphous.

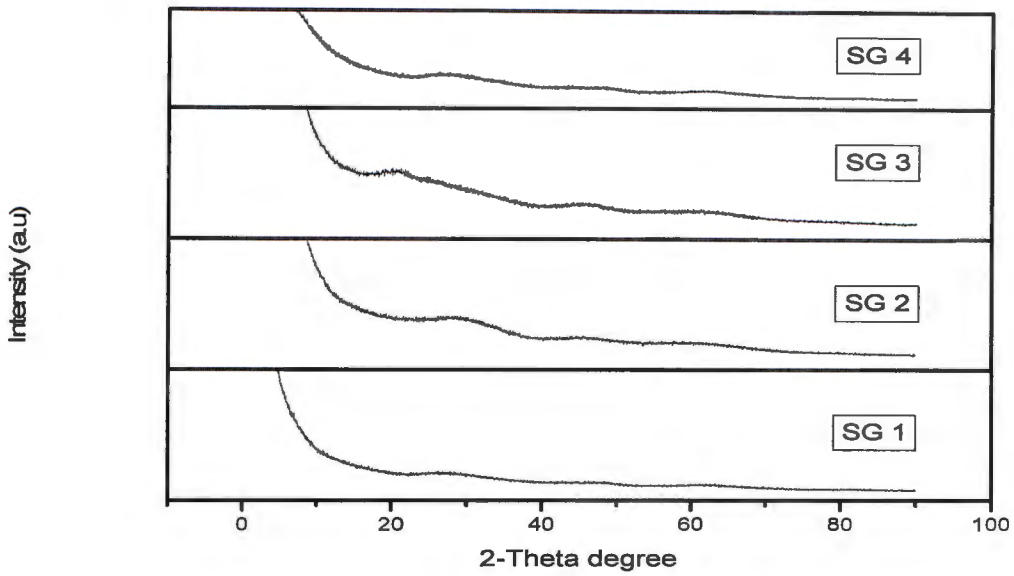

Figure 4.2 XRD patterns of xerogel materials prepared by the sol-gel method

4.3.3 FT-IR

Figure 4.2 shows the FT-IR spectra of TiO_2 structures prepared by the sol-gel method. A broad band observed between 3700 and 3000 cm^{-1} represents the O-H stretching mode of hydroxyl group. This is due to the presence of physically adsorbed water in the sample [4, 5]. The FTIR clearly shows one environment of OH group resulting from physical adsoption of water suggesting that the gel does not contain structural OH groups. All the FTIR spectra show the absorption peaks at 500-600cm^{-1} which can be associated to the vibrational modes of Ti-O-Ti [6]. Both XRD and EDX did not reveal the presence of any contaminants. However, the FTIR figure (4.3) revealed what seems like the graphitic carbon wave number. If this is the case the FTIR contamination must have been attributed during analysis process as this is not expected. Furthermore, this could correspond to any other unknown contaminants. Further studies will be done to determine the nature of this contaminant.

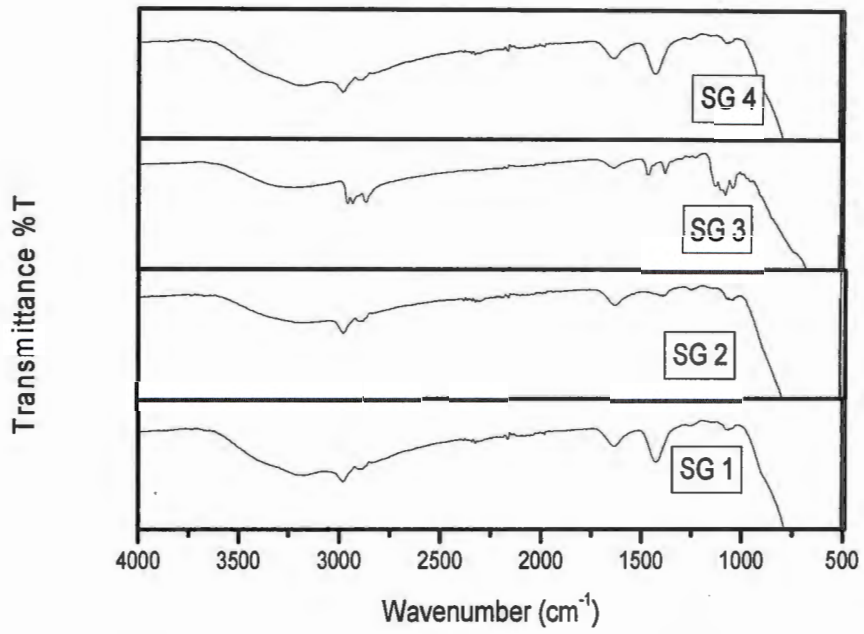

Figure 4.3 FT – IR spectra of xerogel material prepared by the sol-gel method

4.3.4 SEM

The use of bio-alcohols in the preparation of TiO_2 using sol-gel method resulted in the formation of a xerogel with different morphology and size dimensions. The use of aprotic methanol resulted in the formation of particles with irregular spherical shape with the average diameter of 500 μm. Particles obtained here tended to form aggregates. The use of ethanol resulted in the formation of bigger particles (1-2 μm) with mostly an oval shape. Irregular spheres could also be observed but they are much fewer than the oval. Amazingly the use of 1-Butanol resulted in the formation of particles with a wide particle size range (1-10 μm). However, all particles exhibitted an ovel (egg-like) morphology. Particle arrangement formed a regular pattern in that big crystals (10 μm) are often separated by small ones. The use of protic ammonium hydroxide led to the formation of particles with the average diameter of 92 nm forming clusters. Furthermore, the clusters formed a porous structure (Figure 4.4 (d)). The pores have an average diameter of 0.5-1 μm. The cross-section of these pores revealed that the pores have a significant depth (over 10 μm).

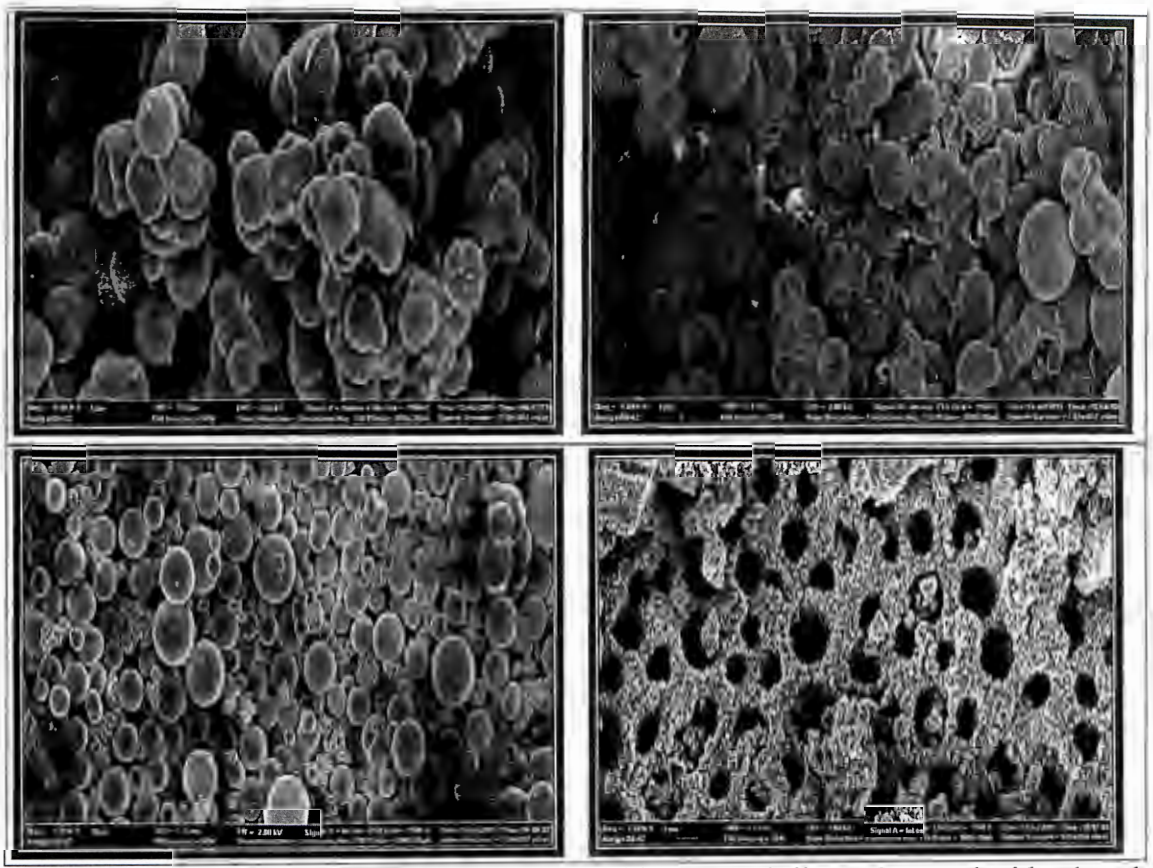

Figure 4.4 (a) SEM pictures of (i) SG 1 treated with methanol (ii) SG 2 treated with ethanol (iii) SG 3 treated with 1-butanol and (iv) SG 4 treated with NH_4OH

4.3.5 TEM

Figures 4.4 (b) show the HRTEM of SG 1 to SG4 samples. TEM revealed more details about the grains and grain boundaries of the particles. Images of figures 4(i) and 4(ii) show that particles are held together by a film at grain boundaries. This could be the reason the pore structure is formed. It could be that particles are strongly bound in a specific manner to form the porous structure.

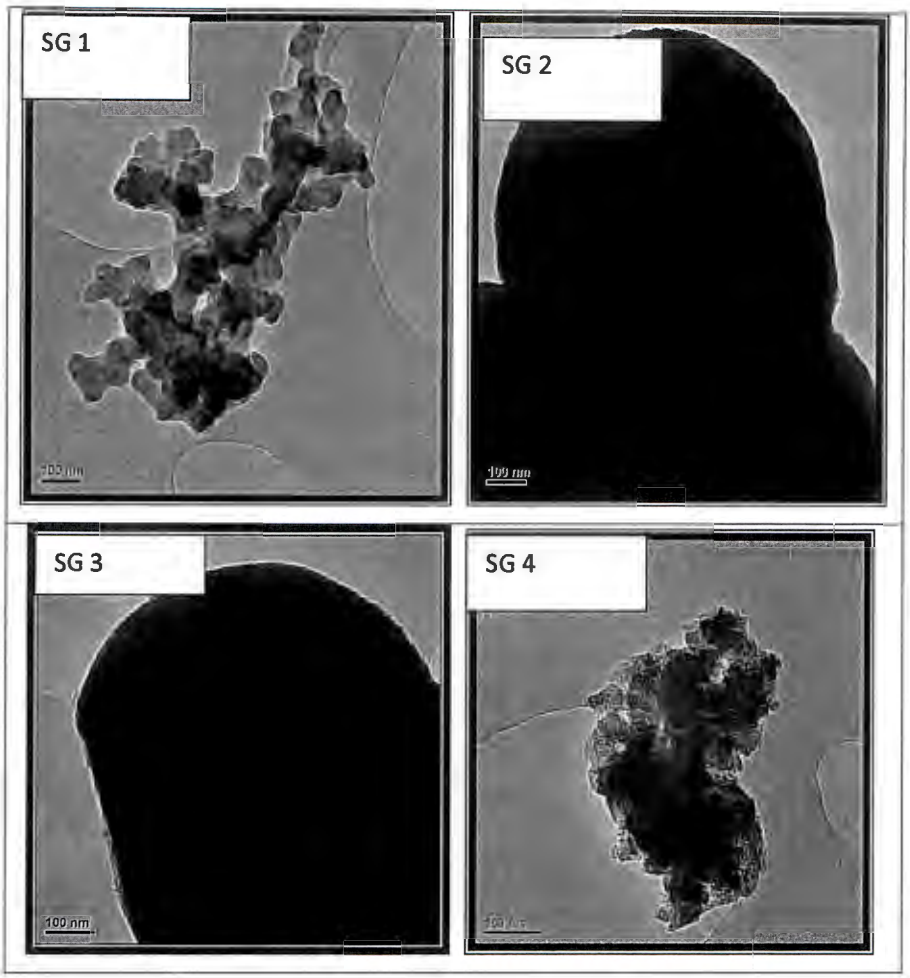

Figure 4.4 (b) (i) TEM pictures of of (i) SG 1 treated with methanol (ii) SG 2 treated with ethanol (iii) SG 3 treated with 1-butanol and (iv) SG 4 treated with NH_4OH

4.4 Discussion

TiO_2 has been synthesized using sol-gel process (literature) before. It is essential to sinter a sol-gel product at high temperature to obtain a crystalline structure. Despite all these visible grains (SEM), all these materials appear to be amorphous (XRD). This is ascribed to xerogel as the materials were not sintered at high temperature. This explains why the XRD peaks corresponding to a TiO_2 structure could not be found. The FTIR clearly shows one environment of OH group resulting from physical adsoption of water suggesting that the gel does not contain structural OH groups.

The SEM data clearly shows that increasing chain length of bio-alcohol leads to a formation of bigger particles with regular oval shape. The difference here is ascribed to alcohol

solubility in water. Both Methanol and Ethanol are completely miscible with water whilst butanol has lower solubility leading to a formation of larger crystals. Thus miscibility decreases with chain length. Interestingly, the use of NH_4OH as a solvent in the sol-gel process led not only to the formation of relatively smaller particles than that obtained in the presence of bio-alcohols but also led to the formation of a porous structure. This is attributed to the difference in pH. NH_4OH is a weak base but certainly more basic than bio-alcohols.

The surface areas of materials produced in the presence of bio-alcohols are relatively comparable but certainly larger than that of Degussa P25 TiO_2. Larger surface area and high porosity of a xerogel are typical phenomenon and this explains why the materials have large surface area. The intra-particle porosity also played a role in the resulting surafce area of the materials. This explains why the materials have larger surface area despite the larger grain sizes (micron sizes). From the FTIR results it is clear that the gel is hygroscopic.

4.5 Conclusion

In this chapter the effect of bio-alcohols on the sol-gel prepared materials was investigated. Based on the results and discussions, the following conclusions were made: xerogel materials could be produced by the sol–gel method using TTP with either a bio-alcohol or an inorganic base as a solvent. The nature and shape of the formed material are largely influenced by the type of solvent used. Thus, increasing the chain length of bio alcohol leads to an increase in particle size. Material prepared with NH_4OH possessed the lowest surface area than the materials prepared from bioalcohols. Therefore, it can be concluded that NH_4OH is a weak solvent compared to the bioalcohols used in this study. Additionally, the use of NH_4OH which is more basic than the bio-alcohols led to the formation of smaller and porous materials. As was expected all the formed materials possessed large surface areas. From the XRD all the materials formed were found to be amorphous.

4.6 References

1. Liu, H., Yang, W., Ma, Y., Cao, Y., Yao, J., Zhang, J., Hu, T., (2003) *Langmuir*: Synthesis and Characterization of titania prepared by using photoassisted Sol-gel method 19 3001 -3005
2. Wang, C. C., and Ying, J., Y., (1999) *Chem. Mater* : Sol-gel synthesis and hydrothermal processing of anatase and rutile titania nanocrystals 11 3113-3120

3. Garcia-Serrano, J., Gomez-Hernandez, E., Ocampo-Fernandez, M., Pal, U., (2009) *Current Applied Physics*: Effect of Ag doping on the crystallization and phase transition of TiO_2 nanoparticles 9 1097-1105
4. Ou, H. H., and Lo, S. L., (2007) *Separation and Purification Technology*: Review of titania nanotubes synthesized via hydrothermal treatment :Fabrication, modification and application 58 179-191
5. Mor, K. G. K., Varghese, O. K., Paulose, Shankar, M. K., Grimes, C. A., (2006) Solar *Energy Materials and Solar Cells*: A review on highly ordered, vertically oriented TiO_2 nanotube arrays: fabrication, material properties and solar energy applications 90, 2011 - 2075
6. Beranek, R., and Kisch, H., (2008) *Photochem. Photobiol. Sci :* Tuning the optical and photoelectrochemical properties of surface-modified TiO_2 7, 40–48

CHAPTER 5

Microwave assisted hydrothermal synthesis of titania derived nanostuctures

5.1 Introduction

TiO_2 nanomaterials can exist in different forms and shapes such as nanorods, nanowires, nanospheres, nanobelts and nanotubes. These features can greatly improve the performance of TiO_2 in many applications [1]. Different applications of these nanomaterials are related to their shape and size. Among these nanostructured materials, titania nanotubes are the most studied. This is because they possess important properties including large surface area, high pore volume, high interfacial charge transfer rate and ion-changeable ability [2, 3, 4]. Methods such as the template method and the anodic oxidation method have been used to prepare titania nanotubes. However, the hydrothermal synthesis has become the most widely used because it is simple and cost-effective. In this chapter the effects of microwave assisted hydrothermal treatment in the synthesis of TiO_2 nanoparticles is reported. Microwave Assisted Hydrothermal Synthesis was chosen because it is faster and more efficient than the conventional hydrothermal treatment as it offers direct delivery of energy to the materials [5]. Thus, in this study xerogel materials prepared in chapter 4 were used as starting materials in the synthesis of tubular structures. To the best of our knowledge there is currently no report on the use of xerogel as the starting material for the preparation of TiO_2 derived nanotubular structures. The objective was to prepare TiO_2 derived nanostructures from a different source like a xerogel and to study the influence it has on the microstructure. In this process the influence of microwave irradiation was investigated.

5.2 Experimental

5.2.1 Preparation of support

A sol-gel prepared sample (xerogel) was mixed with 18 M of KOH with constant stirring. The mixture was transferred into the Teflon vessels and then placed in microwave (Anton Paar- multiwave 3000). The mixture was heated at 150° C for 15 minutes. After being allowed to cool to RT, the resultant mixture was washed with deionized water. The solid particles were separated from the mixture by centrifugation at 4500 rpm for 15 minutes. The

washing was done until conductivity of the sample was less than 100 μS / cm. The product was then dried in an oven for 12 hours and then characterized.

5.2.2 Characterization

The obtained materials were characterized using the techniques outlined in subsection 4.2.2.

5.3 Results

5.3.1 BET

The surface areas for microwave treated materials are given in Table 5.1. The surface areas were decreased compared to the surface areas of the as-prepared materials. This is simply due to material transformation from xerogel to a crystalline form(s) of TiO_2. Also, hydrothermal treatment of titania nanomaterials is known to reduce the surface area of materials [2].

Table 5.1 BET surface areas of microwave prepared samples

Name	Description	Surface Area
MW 1	xerogel / methanol	218 m^2 / g
MW2	xerogel / ethanol	318 m^2 / g
MW3	xerogel / 1-butanol	351 m^2 / g
MW 4	Xerogel / NH_4OH	4 m^2 / g

5.3.2 XRD

Figure 5.1 shows the XRD patterns of materials synthesized hydrothermally using microwave irradiation. The patterns consist of broad peaks that could not be indexed to any known structure. However, studies in the literature have shown that these broad peaks correspond to a titanate structure, $KTiO_2$ (OH), with a layered structure of titanate. It is believed that the broadening is due to size effect of these tubular structures. [6]

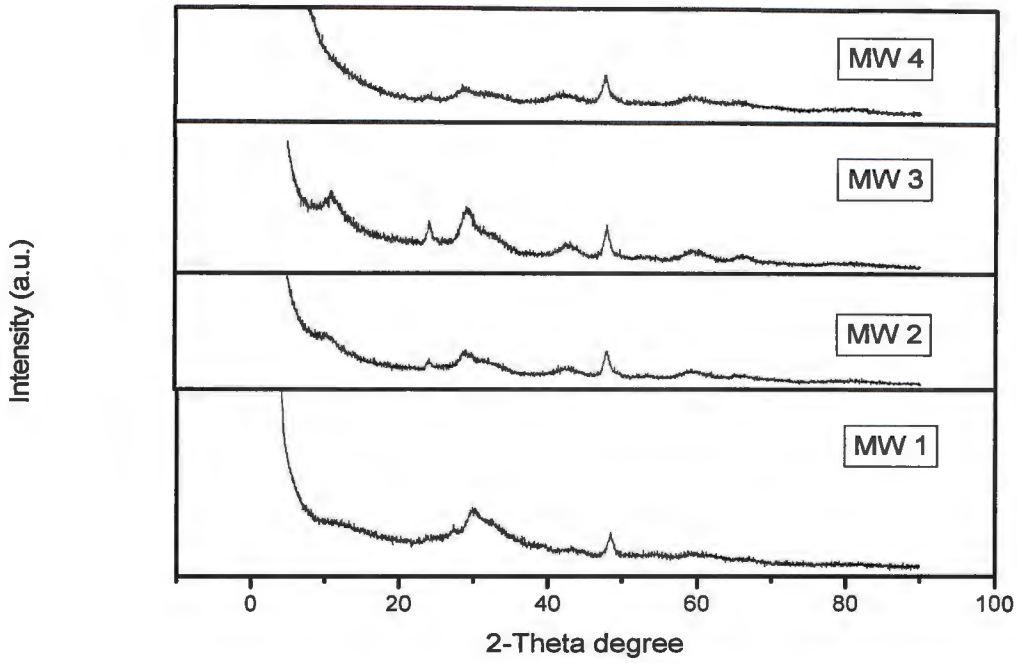

Figure 5.1 XRD patterns of titanate materials prepared by microwave

5.3.3 EDX

Energy-dispersive X-ray spectroscopy (EDX) was analyzed to obtain information about the chemical nature and composition of the sample. The spectrum showed the presence of titanium (Ti) and oxygen (O). The presence of potassium (K) shows that K could not be completely removed from the material even after a long washing process that was done to obtain a conductivity less than 100 μS / cm. The carbon (C) comes from the carbon coating tape that was used as material support.

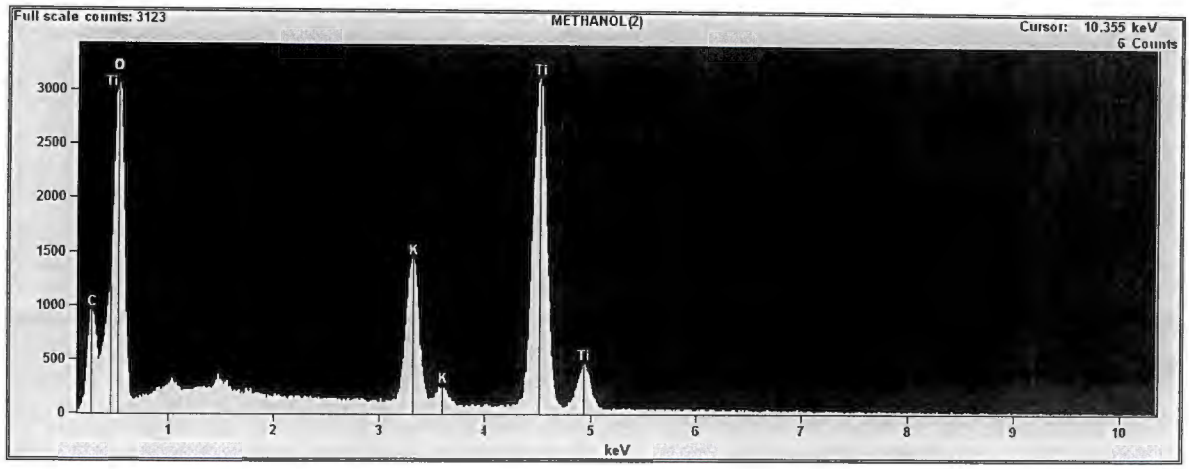

Figure 5.2 EDX spectra of microwave prepared sample showing the presence of potassium

5.3.4 FT-IR

Figure 4.2 shows the FT-IR spectra of TiO_2 structures prepared by the sol-gel method. A broad band observed between 3700 and 3000 cm^{-1} represents the O-H stretching mode of hydroxyl group. This is due to the presence of physically adsorbed water in the sample [3, 4]. The FTIR clearly shows one environment of OH group resulting from physical adsoption of water suggesting that the gel does not contain structural OH groups. The spectra show the absorption peaks at 500-600cm^{-1} which can be associated to the vibrational modes of Ti-O-Ti due to condensation reaction

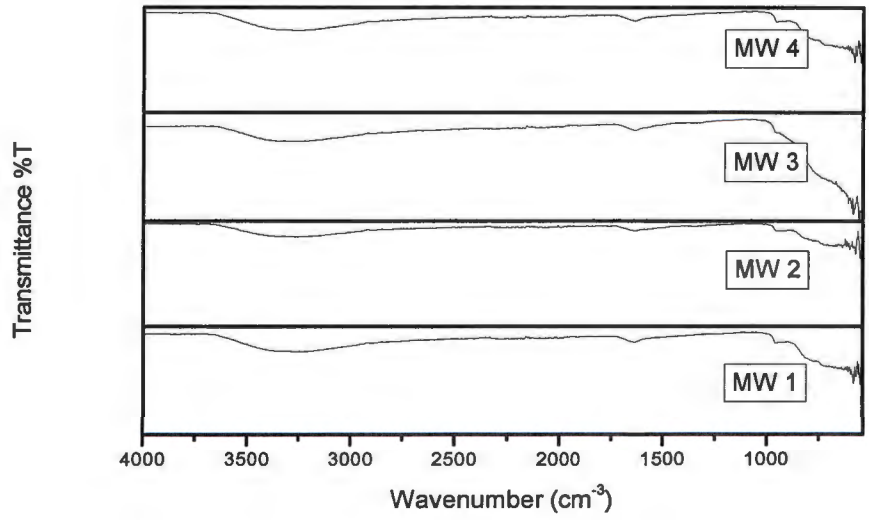

Figure 5.3 FT – IR spectra of titanate materials prepared by microwave

5.3.5 SEM

The results herein revealed that the use of xerogel as starting materials could produce a tubular form of nanomaterials. It is interesting to note that although the xerogels used as starting materials were very different in size, the tubular structures formed have the same size (diameter of 7-12 nm) and all showing a narrow size distribution. MW 1 the tubes appear to be very long and they are randomly distributed. MW 2 tubes are clustered together and are also randomly distributed. MW 3 the tubes appear to be very thin. MW 4 the tubes are too agglomerated and are arranged into what looks like a brain.

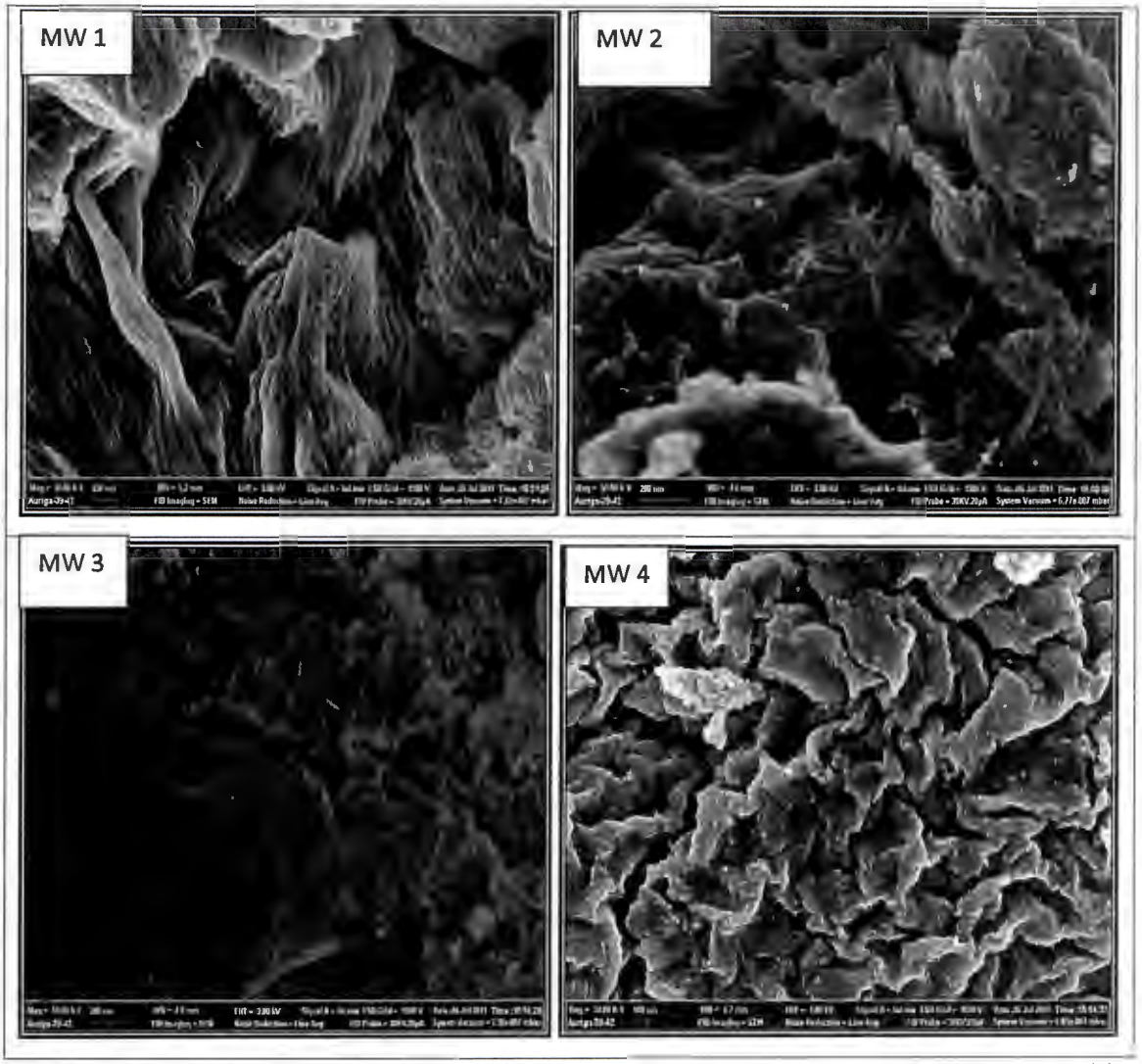

Figure 5.4. (a) SEM pictures of (i) MW 1 treated with methanol (ii) MW 2 treated with ethanol (iii) MW 3 treated with 1-butanol and (iv) MW 4 treated with NH_4OH

5.3.6 TEM

The images below confirm that the formed structures are indeed nanotubes. However, the produced nanotubes were different for different samples. MW 1 and MW 4 showed 100% tube formation, while MW 2 and MW 3 showed tube formation with some unreacted materials.

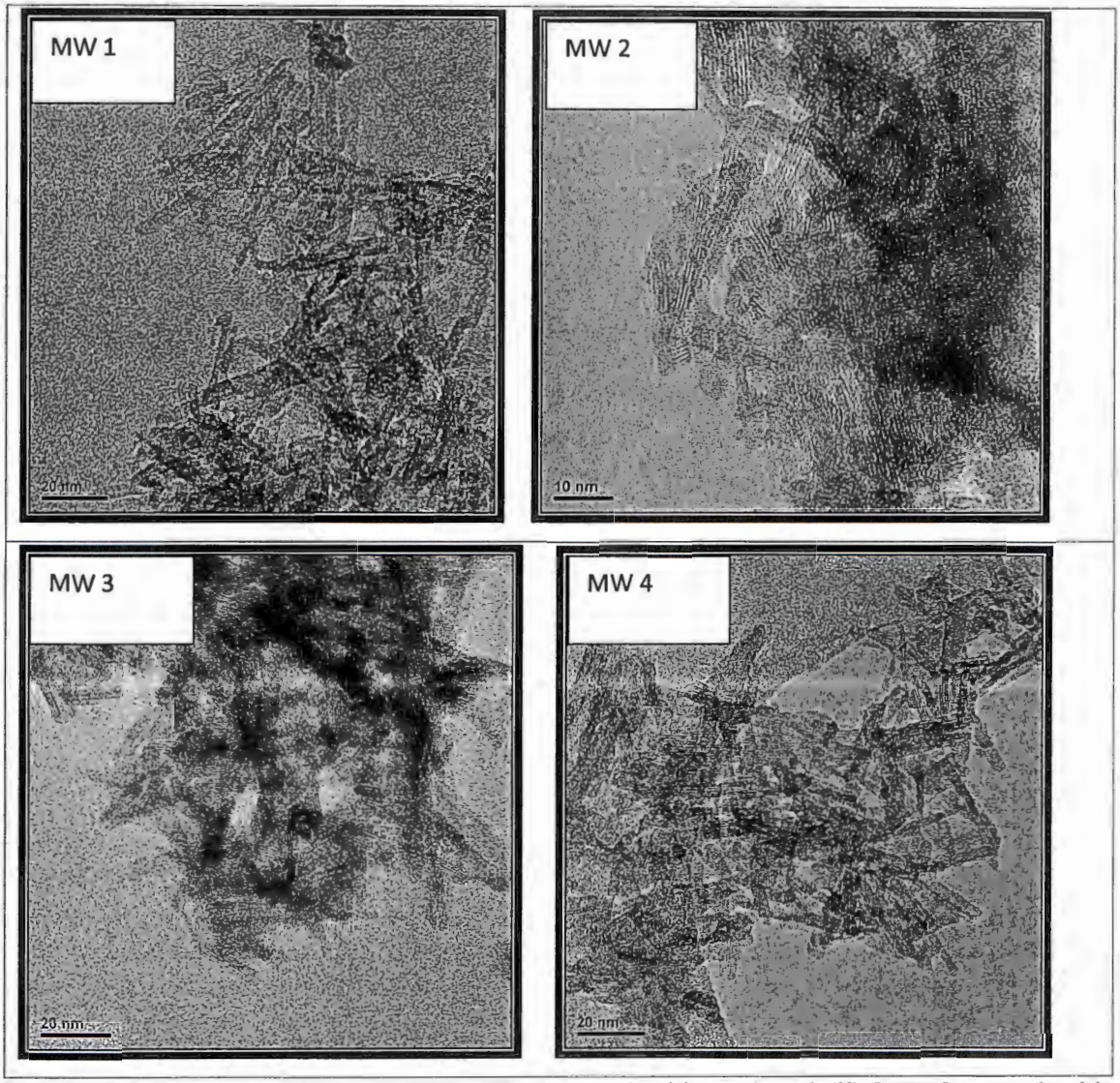

Figure 5.4. (b) TEM pictures of (i) MW 1 treated with methanol (ii) MW 2 treated with ethanol (iii) MW 3 treated with 1-butanol and (iv) MW 4 treated with NH_4OH

5.4 Discussion

The results herein revealed that the use of xerogel as starting materials could produce a tubular form of nanomaterials that are more crystalline than the gel. This is confirmed by the presence of XRD peaks sharper than those of the gel (chapter 4). It is interesting to note that

although the xerogels used as starting materials were very different in size the tubular structures formed have the same size (diameter of 7-12 nm) and all showing a narrow size distribution. However, the surface areas of the tubular structures are different. The surface areas have decreased because generally, xerogels have a large surface area which shrinks upon heat treatment at elevated temperatures. Those of bioalcohols showed an increase with an increase in the chain length. It is interesting to note that the surface area of a base still remained low. Sikhwivhilu and co-workers have shown that hydrothermal processing of P25 Degussa TiO_2 using microwave irradiation leads to a formation of a titanate structure without potassium as part of the structural framework, Ti_3O_7 [7]. However, our studies have revealed that using a xerogel as starting material leads to a formation of a titanate structure of the form $KTiO_2$ (OH). The presence of potassium is confirmed by the EDX spectrum.

5.5 Conclusion

The xerogels prepared by the sol-gel method were successfully transformed into nanotubular materials after microwave–assisted hydrothermal treatment. The formed nanotubes possessed similar particle sizes and the same crystal structures. However, the surface areas of bioalcohols remained higher than the surface area of an inorganic base. Based on the obtained results it is safe to conclude that microwave hydrothermal treatment greatly affects the morphology, particle size, surface area and crystallinity of materials.

5.6 References

1. Qamar, M., Yoon, C. R., Oh, H. J., Lee, N. H., Park, K. Kim, D. H., Lee, K. S., Lee W. J., and Kim, S. J., (2008) *Catalysis Today* : Preparation and photocatalytic activity of nanotubes obtained from titanium dioxide 131 3 -14
2. Wong, C. L., Tan, Y. N., Mohamed, A. R., (2011) *Journal of Environmental Management* : A review on the formation of titania ananotube photocatalysts by hydrothermal treatment 92 1669-1680
3. Ou, H. H., and Lo, S. L., (2007) *Separation and Purification Technology*: Review of titania nanotubes synthesized via hydrothermal treatment :Fabrication, modification and application 58 179-191
4. Mor, K. G. K., Varghese, O. K., Paulose, Shankar, M. K., Grimes, C. A., (2006) *Solar*

Energy Materials and Solar Cells: A review on highly ordered, vertically oriented TiO_2 nanotube arrays: fabrication, material properties and solar energy applications 90 2011 - 2075

5. Oghbaei, M., and Mirzae, O., (2010) *Journal of Alloys and Compounds* : Microwave versus conventional sintering : A review of fundamentals 494 175-189
6. Sikhwivhilu, L. M., Mpelane, S., Mwakikunga, B. W. S. Sinha Ray, S. (2012) *Applied Materials and Interfaces* : Photoluminescence and hydrogen Gas-Sensing properties of titanium dioxide nanostructures synthesized by hydrothermal treatments 4 1656 -1665
7. Sikhwivhilu, L. M., Sinha-Ray, S., Coville, N. J., (2009) *Appl. Phys A*: Influence of bases on hydrothermal synthesis of titanate nanostructures 949 963-973

CHAPTER 6

The effect of phase composition on the formation of tubular structures prepared hydrothermally

6.1 Introduction

Titanium dioxide derived nanotubes (TNT) are particularly interesting, partly because they have a large specific surface area that can enhance their potential in environmental purification, decomposition of carbonic acid gas, and generation of hydrogen gas[1]. Sintering is believed to affect the particle size, surface area, pore volume and structure of titania nanotubes [2]. Treating TiO_2 nanotubes at higher temperatures (i.e sintering) produces a series of phase changes. The evolution of the anatase phase can be induced at 400° C finally developing into a stable rutile phase at temperatures between 600 and 800° C. The exact temperature depends on the source and preparation history of the nanotubes [3]. Additionally, an increase in temperature can also lead to denaturing of tubes and structural transformations. For example, depending on one's starting material if one start off from a metal-ion containing structure like $KTiO_2$ (OH) one may end up with another form of titanate structure but not necessarily a TiO_2. This chapter focuses on the effect of phase composition on the formation of tubular structures prepared by hydrothermal method.

6.2 Experimental

6.2.1 Procedure

Two of the samples prepared by sol-gel method (SCM 1 and SCM 2) were calcined at 400 °C for 3 hours and then characterised before they were treated hydrothermally in a microwave reactor unit. In order to control the phase composition of the materials four samples already treated (uncalcined) in a microwave were only calcined after this treatment (CMW). All samples were subsequently characterized using techniques described in section 4.2.2.

6.3 Results

6.3.1 SEM

Figure 6.4 shows the SEM images of materials that were calcined after microwave assisted hydrothermal treatment. These images revealed that the morphology of the materials that were calcined after hydrothermal treatment did not change. However, calcining at 400 °C caused the materials to be more aggregated to one another. The particle sizes showed a slight

increase of about 16-24 nm. The material prepared with 1-butanol still formed ball-like structures. However, the ball-like structures in this case are bigger and this was suspected to be due to agglomeration [4]. Materials that were calcined prior to microwave treatment formed nanotubes that were also agglomerated. The particle sizes were comparable to those obtained from calcinations after microwave treatment.

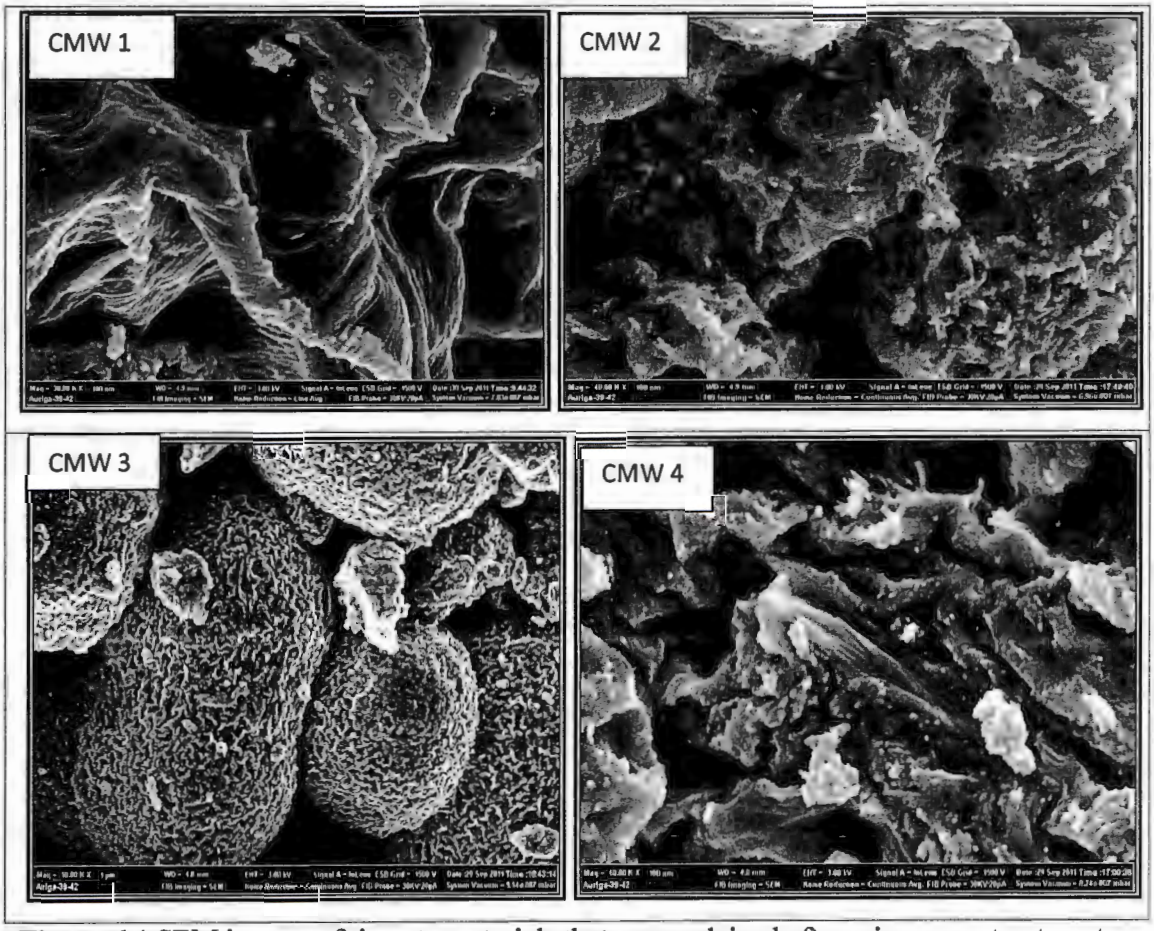

Figure 6.1 SEM images of titanate materials that were calcined after microwave treatment

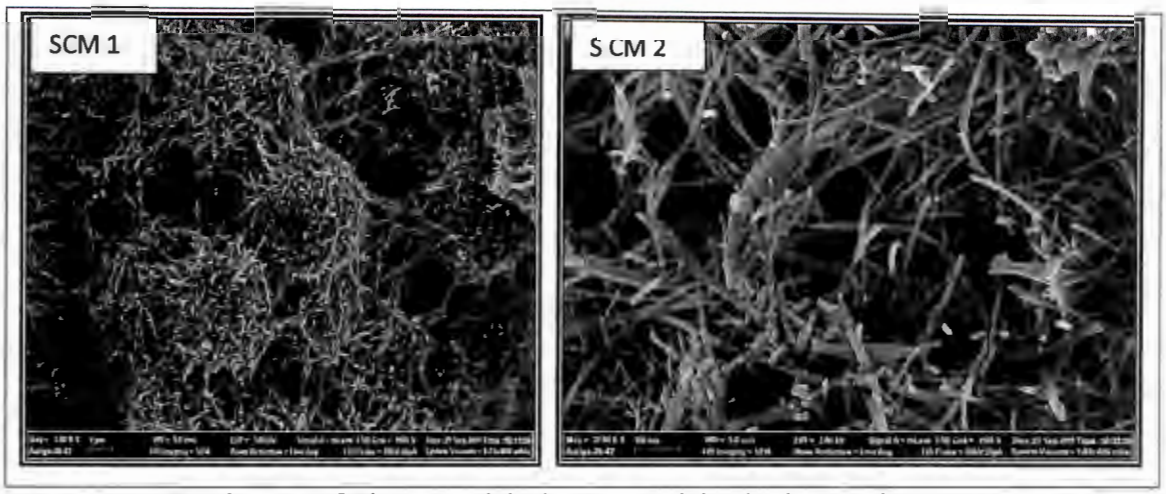

Figure 6.2 SEM images of TiO_2 materials that were calcined prior to microwave treatment

6.3.2 BET

The surface areas for CMW and SCM prepared materials are shown in tables 1 and 2 respectively. The BET results show that the surface areas for both methods were considerably decreased. This further confirms that sintering decreases the surface areas of materials, suggesting further grain growth as was confirmed by the diameter sizes calculated from the SEM images. However, the CMW materials had larger surface areas than the SCM materials. This suggests that the sintering stage plays a role in the surface areas of nanomaterials.

Table 1. BET surface areas of materials that were calcined after microwave treatment

Name	Description	Surface Area
CMW 1	xerogel / methanol	257 m^2 / g
CMW2	xerogel / ethanol	308 m^2 / g
CMW3	xerogel / 1-butanol	262 m^2 / g
CMW 4	xerogel / NH_4OH	261 m^2 / g

Table 2. BET surface areas of sol-gel prepared materials that were treated under microwave after calcinations

Name	Description	Surface Area
SCM 1	xerogel / 1-butanol	190 m^2 / g
SCM 2	xerogel / NH_4OH	82 m^2 / g

6.3.3 XRD

The XRD patterns for materials that were calcined after microwave treatment are shown in figure 6.1. It is interesting to note that even after calcination at 400 °C, materials were similar to those obtained from microwave treatment (chapter 5) suggesting that there is no structural change. This means that the tubes are thermally stable up to 400 °C. However, the peaks are more defined suggesting particle growth. These results are in agreement with the SEM results which showed that there was an increase in diameter sizes. Figure 6.2 shows the XRD patterns of sol-gel prepared samples that were calcined at 400 °C prior to microwave assisted hydrothermal processing, SCM 1 and SCM 2. Their peaks are sharper with high intensities. This is indicative of improved crystallinity of materials. Both SCM 1 and SCM 2 showed peaks that could be indexed to anatase phase. The peaks were narrower indicating that anatase is a crystalline phase.

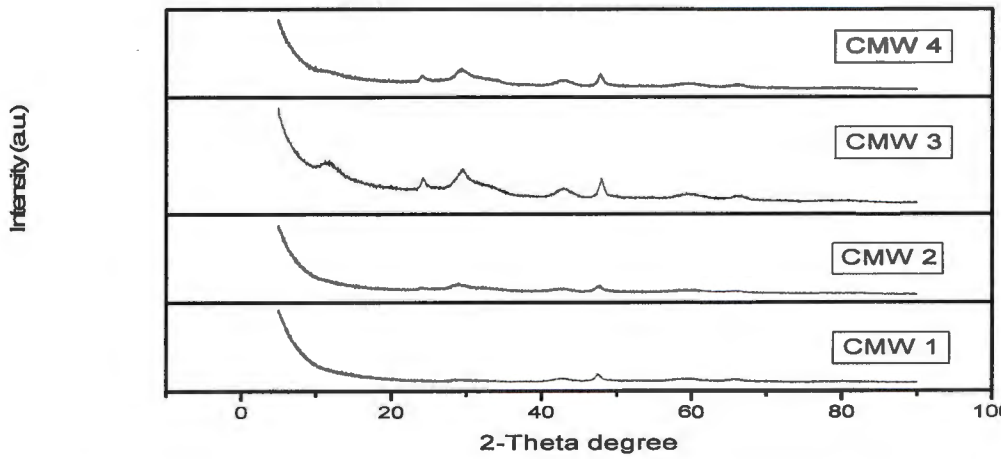

Figure 6.3 XRD patterns of materials that were calcined after microwave treatment

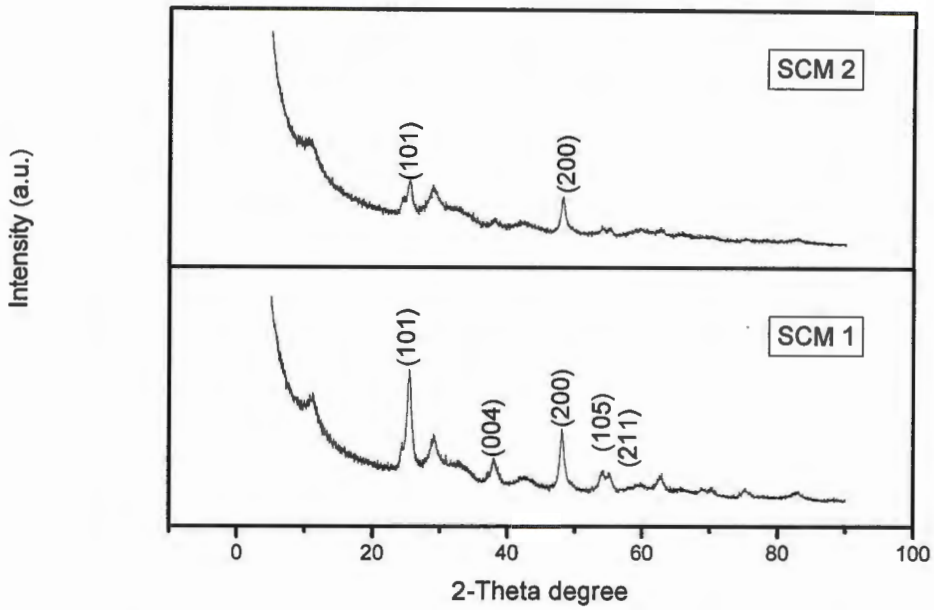

Figure 6.4 An indexed XRD pattern of materials that were calcined prior to microwave treatment [5, 6]

6.4 Discussion

The surface areas for both materials (materials calcined after microwave treatment and materials calcined prior to microwave treatment) decreased after calcination. This is ascribed to phase transformation. I.e. calcination of material prior to microwave treatment led to the transformation from xerogel to a crystalline structure accompanied by morphological transformation from irregular spheres to tubular structures. The formation of anatase TiO_2 for both SCM 1 and SCM 2 clearly shows that, depending on the starting materials, a phase pure material could be achieved. It is clear that the nature and phase content of the starting materials play an important role in the formation of the product. The SEM pictures revealed that the morphology of the materials that were calcined after microwave treatment did not change i.e they remained tubular. However, calcining materials at 400° C led to particle growth by Ostwald ripening. This is a phenomenon where small crystals dissolve and redeposit onto larger ones. An increase in particle sizes is indicative of crystal growth induced by thermal treatment [7]. The similarity in XRD patterns to those obtained from microwave treatment (chapter 5), means that the tubes are thermally stable up to 400 ° C. However, the peaks are more defined suggesting particle growth. These results are in agreement with the SEM results which showed that there was an increase in diameter sizes.

An increase in diameter size was further confirmed by a decrease in surface areas of the materials. However, microwave treatment of calcined materials led to the formation of tubes with comparable size dimension. This implies that the size of tubes is largely influenced by method and conditions of preparation.

6.5 Conclusion

It is evident that calcination stage is very important on the particle size, morphology; surface area and structure of titanate nanotubes. Samples treated with Microwaves prior to calcination have proven to be more thermally stable than those calcined first before being subjected to microwave irradiation. The surface areas of these thermally stable materials also remained higher than those of materials calcined prior to microwave treatment. The nature of starting materials influences the structure of the formed products. Materials calcined prior to microwave treatment produced an anatase material.

6.6 References

1. Sikhwivhilu, L. M., Mpelane, S., Mwakikunga, B. W., Sinha Ray, S., (2012) *Applied Materials and Interfaces* : Photoluminescence and hydrogen Gas-Sensing properties of titanium dioxide nanostructures synthesized by hydrothermal treatments 4 1656 - 1665
2. Qamar, M., Yoon, C. R., Oh, H. J., Lee, N. H., Park, K., Kim, D. H., Lee, K. S., Lee, W. J., Kim, S. J., (2008) *Catalysis Today* : Preparation and photocatalytic activity of nanotubes obtained from titanium dioxide 131 3 -14
3. Jaroenworaluck, A., Regonini, D., Bowen, C. R., Stevens, R., (2010) *Applied Surface Science A* : microscopy study of the effect of heat treatment on the structure and properties of anodised TiO_2 nanotubes 256 2672–2679
4. Wong, C. L., Tan, Y. N., Mohamed, A. R., (2011) *Journal of Environmental Management* : A review on the formation of titania ananotube photocatalysts by hydrothermal treatment 92 1669-1680
5. Zou. Y., Wang. Z., Lan. X., Huang. N., and Wang. C., (2009) *Journal of the Korean Physical Society*: Anatase phase TiO_2 anode of a dye – sensitized solar cell prepared by using RMFMS 55 2650 - 2653

6. Parmar. K. P. S., Ramasamy. E., Lee. J. W., and Lee J. S., (2010) *Scripta Materialia*: A simple method for producing mesoporous anatase TiO_2 nanocrystals with elevated photovoltaic performance 62 223 - 226
7. Sikhwivhilu, L. M., S. Sinha-Ray, S., Coville, N. J., (2009) *Appl. Phys A*: Influence of bases on hydrothermal synthesis of titanate nanostructures 949 963-973

CHAPTER 7

Preparation of composite materials with antibacterial properties

7.1 Introduction

The impregnation of noble metals on the surface of a support material has proven to improve on the activity and stability of the support. Supports that are usually used include TiO_2, SiO_2 and Al_2O_3 [1]. Silver loaded TiO_2 nanocomposites have attracted a great deal of attention due to unique electronic and optical properties of TiO_2 and good antibacterial properties of silver [1,2]. Silver is known to enhance the photocatalytic efficiency of TiO_2 for organic contaminant degradation and bacterial inactivation. Silver-coated titanium dioxide photocatalysts have have been studied by many researchers which showed that the morphology of the deposited silver particles depends on the type of titanium dioxide used as support material [3]. In this chapter we have used two different supports (the spherical xerogel and tubular titanate material) to study how the morphology and structure of support could influence the size, shape and dispersion of Ag nanoparticles.

7.2 Experimental

7.2.1 Silver loading

Two samples (xerogel material prepared by sol-gel method and the nanotubular material prepared by microwave assisted hydrothermal treatment) were loaded with silver using wet-impregnation method. During the synthesis TiO_2 powder was immersed in 5wt % silver nitrate. The prepared $AgNO_3$ / TiO_2 nanopowder was aged at room temperature overnight and then dried at 100°C until it was completely dry. Then the samples were calcined at 300°C for 4 hours. This was done to remove the nitrate moiety.

7.2.2 Characterization of TiO_2 nanostructures

The obtained nanomaterials i.e the xerogels obtained from sol-gel (SM) and the nanotubular materials (TM) obtained from microwave assisted hydrothermal treatment were characterized using techniques outlined in subsection 4.2.2.

7.3 Results

7.3.1 BET

The inclusion of silver on the tubular materials followed by sintering at 300 °C led to a decrease in surface area as shown in table 7.1. A decrease in surface area was suspected to be due to sintering and this suggests that silver had no effect on the surface areas of the resultant materials. These results are similar to those obtained in the literature [2] where silver showed no effect on the surface area after being loaded into TiO_2.

Table 7.1: The surface areas of spherical xerogel and tubular titanate materials impregnated with silver

Name	Description	Surface Area
AgL 1	TM	233.0728 m^2 / g
AgL 2	SM	111 m^2 / g

7.3.2 XRD

Figure 7.1 shows the XRD patterns of spherical xerogel and tubular titanate materials loaded with silver. No silver peaks could be observed on the XRD pattern. This could mean that the amount of silver was too low to be detected by the XRD. However, the successful loading of silver on the surface of TiO_2 was confirmed by the TEM images and EDX spectrum. Nonetheless, AGL2 showed an improved crystallinity with a high intensity anatase peak than AGL 1. The difference in crystallinity was suspected to be due to the nature of materials used as was proven in the previous chapter.

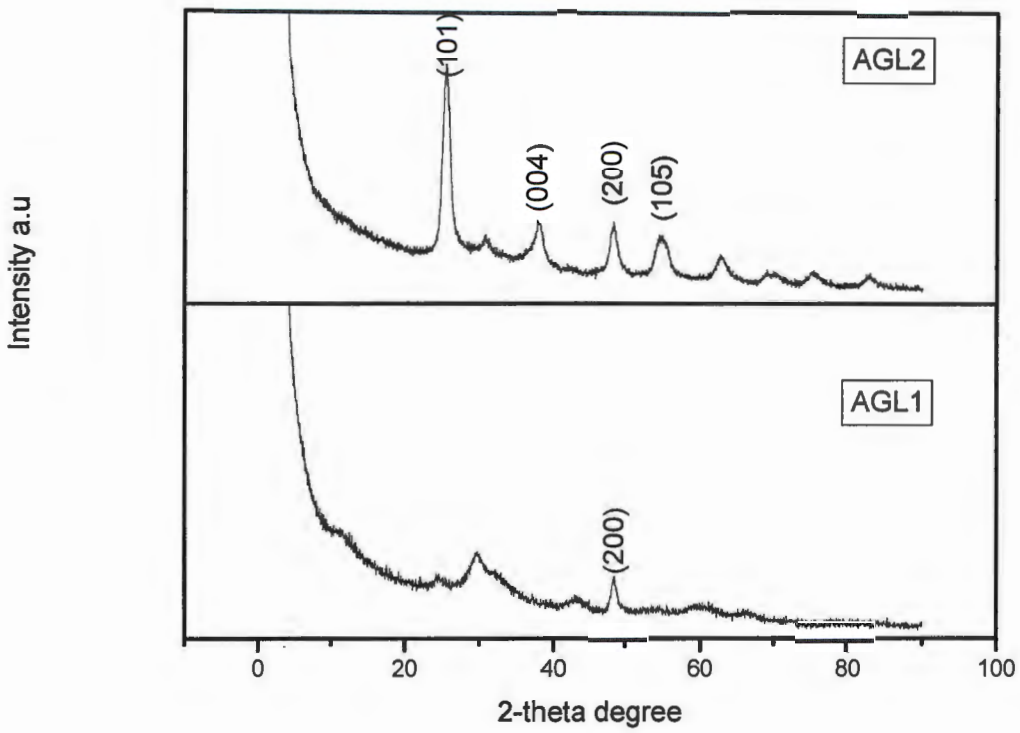

Figure 7.1 XRD patterns of silver loaded materials [4]

7.3.3 EDX

EDX analysis shows the presence of silver in the materials, thereby confirming the successful loading of silver in the titania materials. The spectrum showed the presence of titanium (Ti) and oxygen (O). Potassium K originates from the treatment with KOH during microwave treatment. The carbon (C) originates from the carbon coating tape used as the sample support.

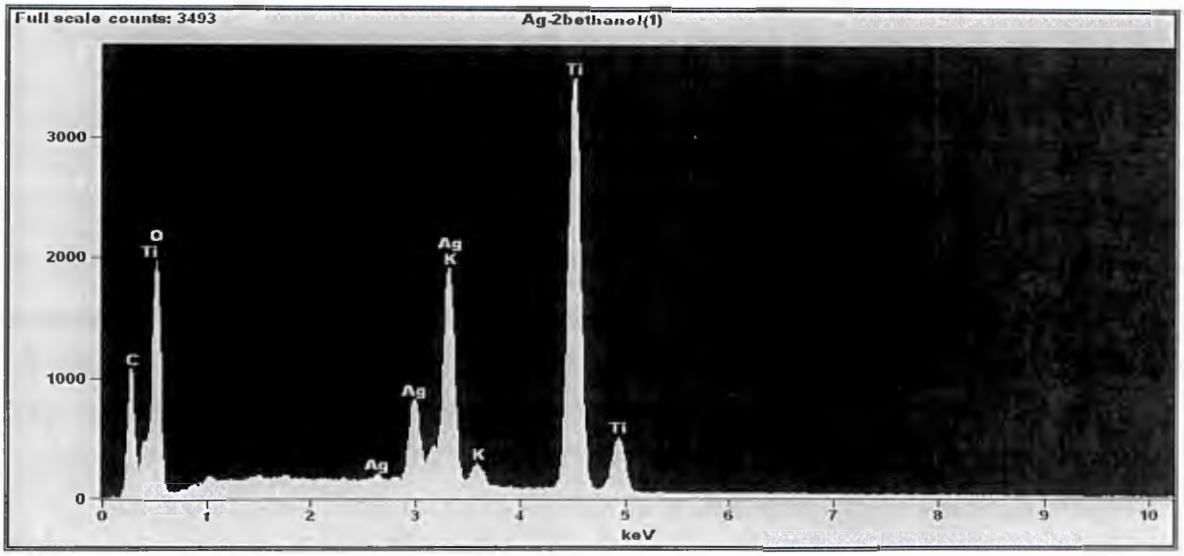

Figure 7.2 EDX spectra of silver loaded materials

7.3.4 TEM

The TEM images of the prepared samples (AgL1 and AgL2) are shown Fig. 7.3. The micrographs show similar microstructures (of silver nanoparticles) for AgL1 and AgL2. Both samples have comparable shapes of silver nanoparticles (represented by dark spots on the samples). It is interesting to note that although silver nanoparticles of AgL1 and AgL2 have similar shapes they have different surface areas (233 and 111 m^2/g, respectively). The surface areas are also different to that of P25 Degussa TiO_2. Furthermore, the material pore diameters are also comparable. The decrease in surface areas of modified samples (AgL1 and AgL2) is probably due to particle growth expedited by thermal treatment.

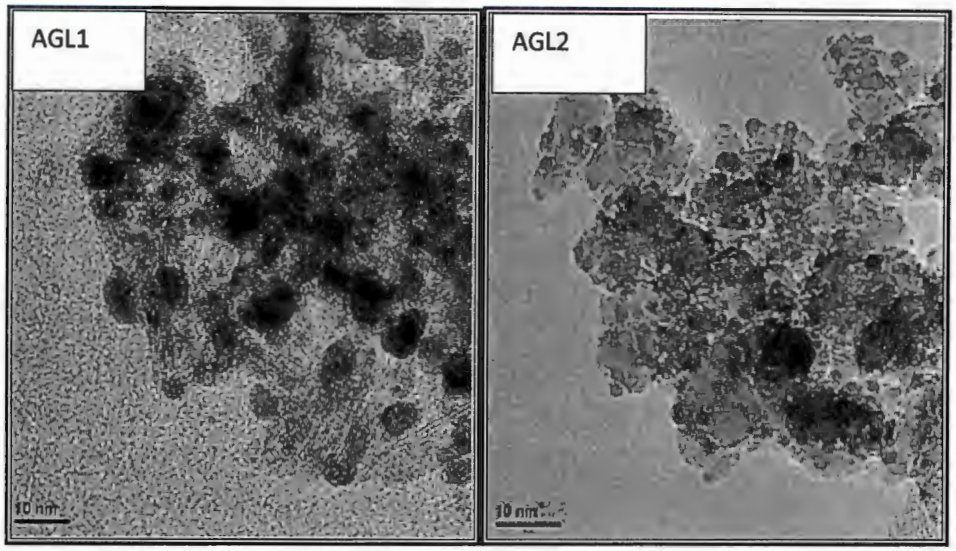

Figure 7.3. TEM images of spherical xerogel and tubular titanate materials loaded with silver materials

7.4 Discussion

In table 7.1 the textural data for the samples are summarized. The specific surface area of the titanate material AgL1 was two times more than that of AgL2. The deposition of Ag on both materials did not significantly alter the features of the support. Average Ag particle sizes of 3 and 5 nm were attained when 5 % Ag was added to titania derived supports (AgL1 and AgL2, Figure. 7.3). The difference in surface area appears to influence the dispersion of Ag. The morphology should lead to good interaction between the support and the metal catalyst that could, for example, limit sintering. This in turn, may have benefits for the durability of supported Ag catalysts, an aspect which has been often neglected in much research work reported to date.

7.5 Conclusion

Silver was successfully deposited on the surfaces of different support materials (spherical and tubular). Material with a large surface area resulted in large particle sizes and a good dispersion of silver nanoparticles.

7.6 References

1. Garcia-Serrano, J., Gomez-Hernandez, E., Ocampo-Fernandez, M., Pal, U., (2009) *Current Applied Physics*: Effect of Ag doping on the crystallization and phase transition of TiO_2 nanoparticles 9 1097-1105
2. Zielinska, A., Kowalska, E., Sobczak, J. W., Lacka, I., Gazda, M., Ohtani, B., Hupka, J., and Zaleska, A., (2010) *Separation and Purification Technology:* Silver-doped TiO2 prepared by microemulsion method 72 309-318.
3. Li-Yuan, C., Shun-wen, W., Beng, P., Zhu-ying, L., (2008) *Trans. Nonferrous Met. Soc. China* : Effect of thermal treating temperature on characteristics of silver doped titania 18 980-985
4. Chen. S., and Carroll. D. L., (2002) *Nano Letters*: Synthesis and characterization of truncated triangular silver nanoplates 2 1003 - 1007

CHAPTER 8

General conclusions and recommendations

8.1 General conclusions

- TiO_2 materials were successfully synthesized by the sol-gel method using different solvents (bioalcohols or an inorganic base). Characterization techniques proved that the use of different solvents results in different morphologies, particle size and different surface areas.
- TiO_2 materials were successfully transformed into titanate nanotubes by microwave assisted hydrothermal method.
- Microwave prepared materials showed thermal stability as they showed no structural change after calcination.
- The starting material determines the final structure of the products. A phase pure TiO_2 could be obtained after calcining the sol-gel prepared materials before treating them under microwave.
- Different morphologies were used as supports for Ag. Nanotubular materials proved to be better supports than the spherical materials due to their large surface areas
- Finally, it can be concluded that the properties of TiO_2 can be controlled by the starting material and the method of synthesis

8.2 Recommendations

The role of NH_4OH on the synthesis of TiO_2 materials should be studied further. The use of this inorganic base at different concentrations will offer a better understanding of its role on the formation of pores on TiO_2. Further work on the role of bio-alcohols on the formation of TiO_2 materials would also be necessary. Comparing the effect of bio-alcohols by employing secondary or tertiary bio-alcohols will offer a better understanding on the role of the type and chain length of bio-alcohol used in the TiO_2 material. Re-calcination of materials that were calcined after sol-gel treatment before being treated by microwave would add on the studies carried out on this work and would also give more depth on the calcination stages of TiO_2 materials.